US006517489B1

(12) **United States Patent**
Phillips et al.

(10) **Patent No.: US 6,517,489 B1**
(45) **Date of Patent: Feb. 11, 2003**

(54) **METHOD AND APPARATUS FOR FORMING MEDICAL ULTRASOUND IMAGES**

(75) Inventors: **Patrick J. Phillips**, Sunnyvale, CA (US); **Kutay F. Ustuner**, Mountain View, CA (US); **Charles E. Bradley**, Burlingame, CA (US); **Lewis J. Thomas**, Palo Alto, CA (US); **David J. Napolitano**, Pleasanton, CA (US)

(73) Assignee: **Acuson Corporation**, Mountain View, CA (US)

(*) Notice: Subject to any disclaimer, the term of this patent is extended or adjusted under 35 U.S.C. 154(b) by 0 days.

(21) Appl. No.: **09/839,709**

(22) Filed: **Apr. 19, 2001**

Related U.S. Application Data

(63) Continuation-in-part of application No. 09/518,972, filed on Mar. 16, 2000, now Pat. No. 6,309,356.

(51) **Int. Cl.**[7] **A61B 8/14**
(52) **U.S. Cl.** **600/458**
(58) **Field of Search** 600/437, 458, 600/472

(56) **References Cited**

U.S. PATENT DOCUMENTS

4,550,607 A 11/1985 Maslak et al.
4,817,434 A * 4/1989 Anderson 73/625
5,573,001 A 11/1996 Petrofsky et al.
5,685,308 A 11/1997 Wright et al.
5,833,613 A * 11/1998 Averkiou et al. 600/440
5,833,614 A * 11/1998 Dodd et al. 600/447
5,891,038 A * 4/1999 Seyed-Bolorforosh et al. .. 600/447
5,924,986 A 7/1999 Chandler et al.
6,309,356 B1 * 10/2001 Ustuner et al. 600/443

OTHER PUBLICATIONS

"Realization of Sinc Waves in Ultrasound Imaging Systems", Mok–Kun Jeong, Sung–Jae Kwon, Tae–Kyong Song and Moo–Ho Bae, Ultrasonic Imaging 21, 173–185 (1999).
"Experimental Study of High Frame Rate Imaging with Limited Diffraction Beams", Jian–yu Lu, IEEE Transactions on Ultrasonics, Ferroelectrics, and Frequency Control, vol. 45, No. 1, Jan. 1998.
"Real–time 3–D Ultrasound Imaging Using Sparse Synthetic Apertue Beamforming", Geoffrey R. Lockwood, James R. Talman and Shelby S. Brunke, IEEE Transactions on Ultrasonics, Ferroelectrics, and Frequency Control, vol. 45, No. 4, Jul. 1998.
"Generation of Sinc Wave by a One–Dimensional Array for Applications in Ultrasonic Imaging", Mok Keun Jeong, Tae Kyong Song, Song Bai Park and Jong Beom Ra, IEEE Transactions on Ultrasonics, Ferroelectrics, and Frequency Control, vol. 43, No. 2, Mar. 1996.

* cited by examiner

Primary Examiner—Francis J. Jaworski
Assistant Examiner—William C. Jung

(57) **ABSTRACT**

A medical ultrasonic imaging method uses transmitted plane waves, or transmitted wavefronts that are substantially planar, to improve contrast agent imaging by generating peak pressures that are more uniform over depth. Depending on the type of contrast agent, the returned frequencies of interest, and the desired strength of the non-linear response, multiple wavefronts can be generated at substantially the same time to increase peak pressures.

10 Claims, 21 Drawing Sheets

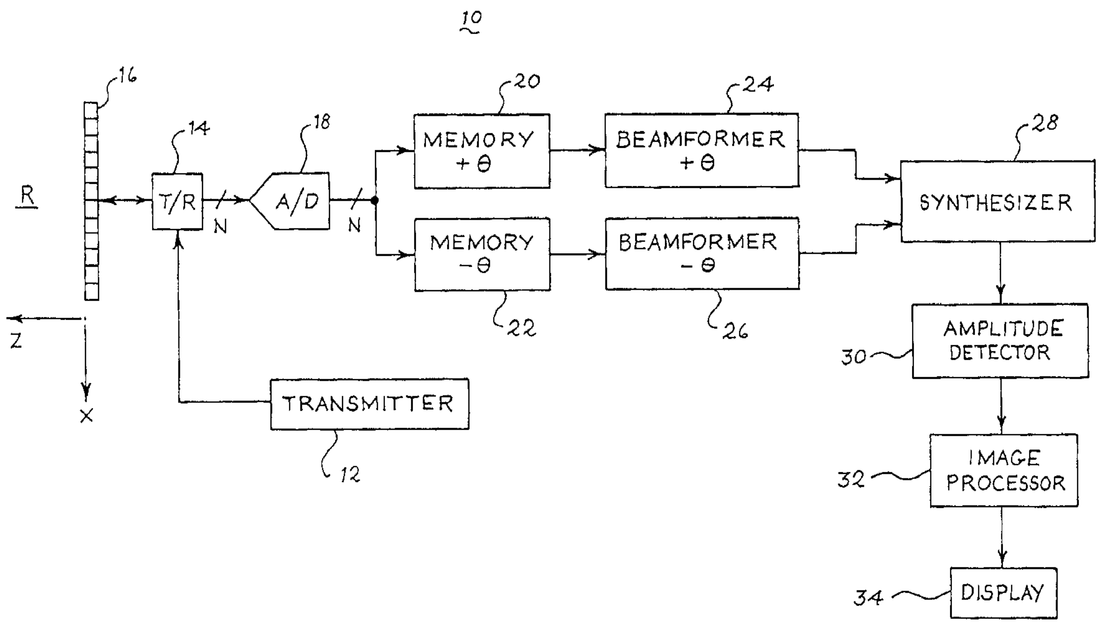

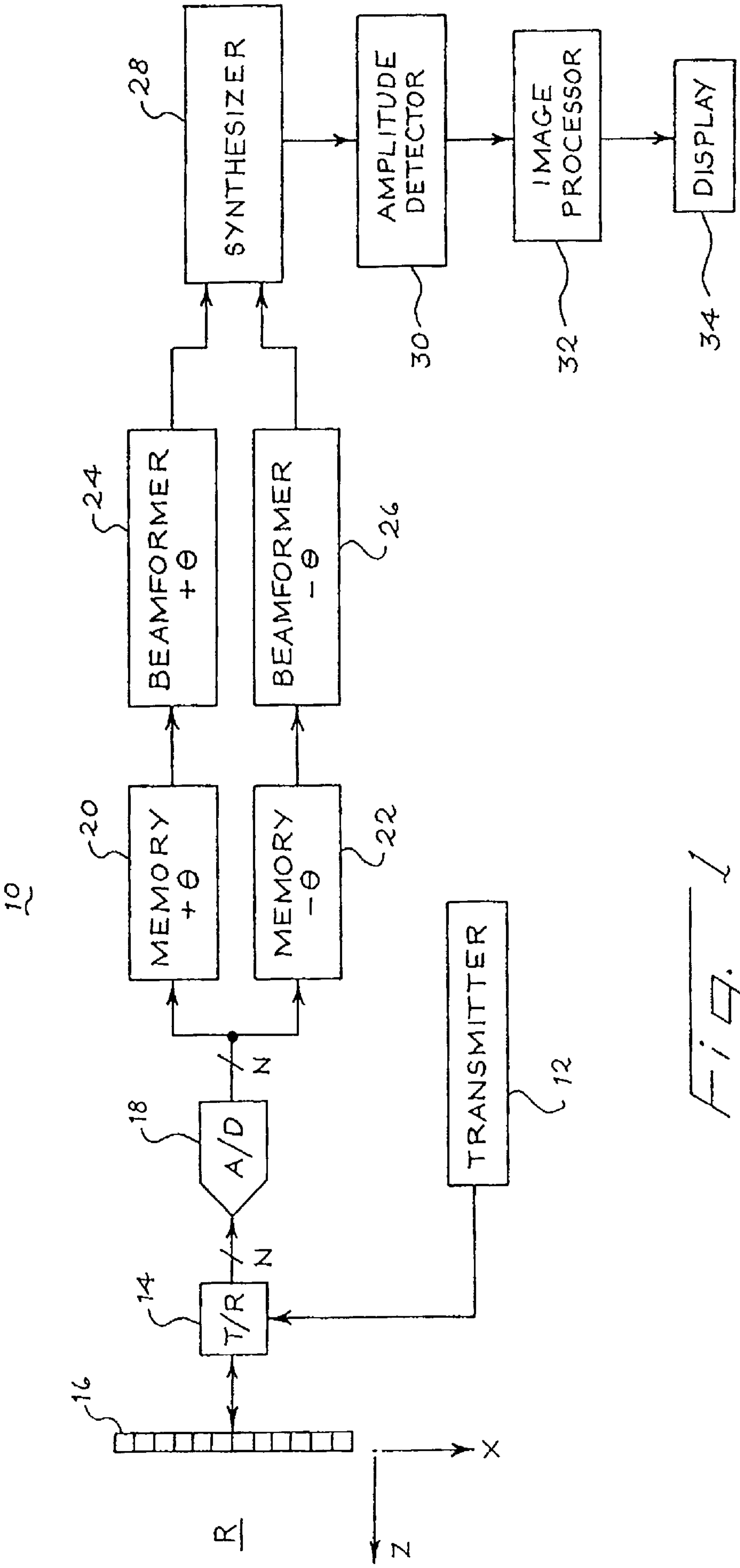
10
SYNTHESIZER
28
AMPLITUDE DETECTOR
30
IMAGE PROCESSOR
32
DISPLAY
34
BEAMFORMER +θ
24
BEAMFORMER −θ
26
MEMORY +θ
20
MEMORY −θ
22
A/D
18
N
N
T/R
14
TRANSMITTER
12
16
R
X
Z

Fig. 1

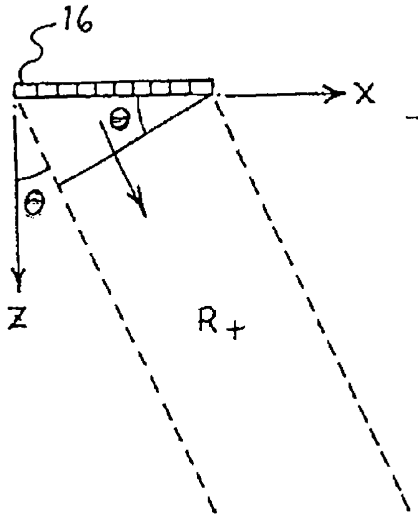

Fig. 2(a)

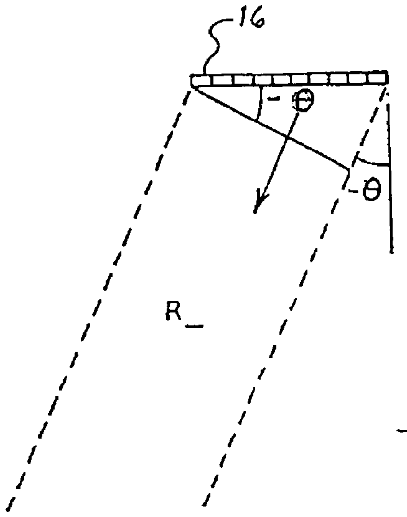

Fig. 2(b)

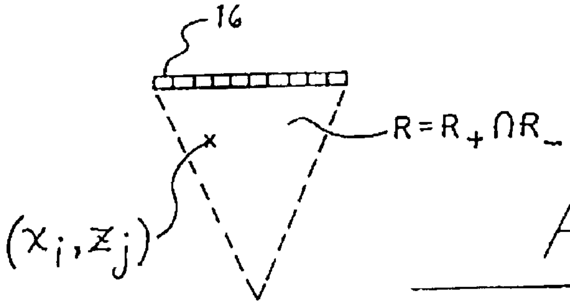

Fig. 2(c)

Fig. 3

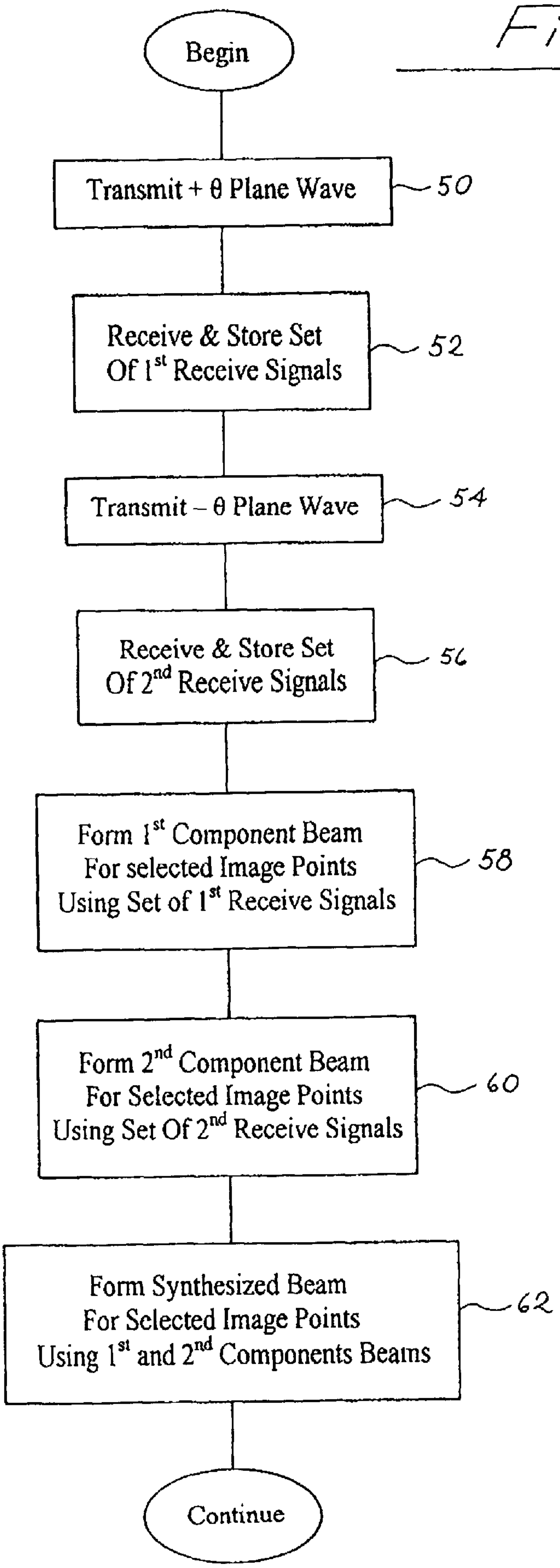
Begin
Transmit + θ Plane Wave
50
Receive & Store Set Of 1st Receive Signals
52
Transmit – θ Plane Wave
54
Receive & Store Set Of 2nd Receive Signals
56
Form 1st Component Beam For selected Image Points Using Set of 1st Receive Signals
58
Form 2nd Component Beam For Selected Image Points Using Set Of 2nd Receive Signals
60
Form Synthesized Beam For Selected Image Points Using 1st and 2nd Components Beams
62
Continue

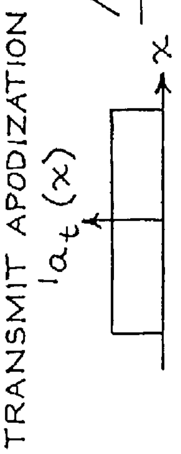

Fig. 4

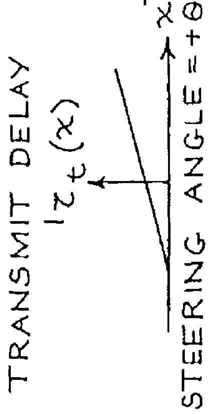

Fig. 5

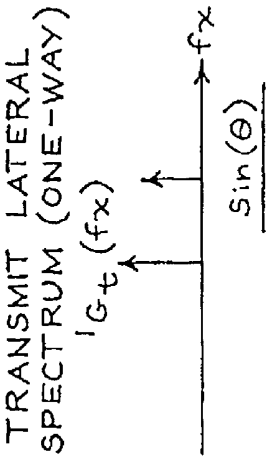

Fig. 6

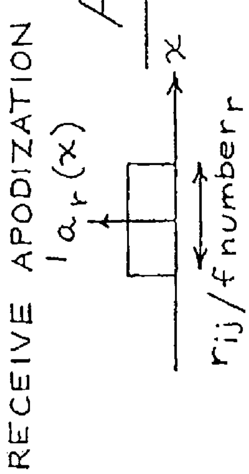

Fig. 7

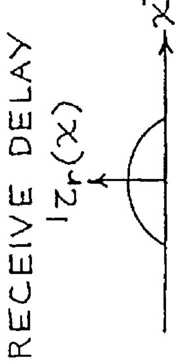

Fig. 8

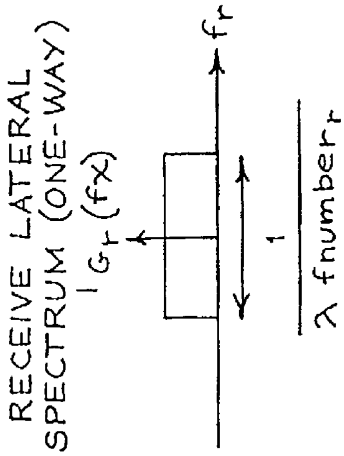

Fig. 9

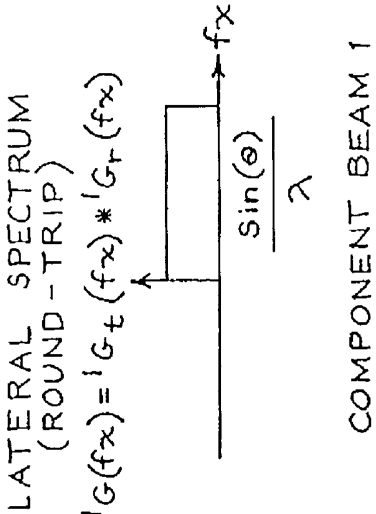

Fig. 10

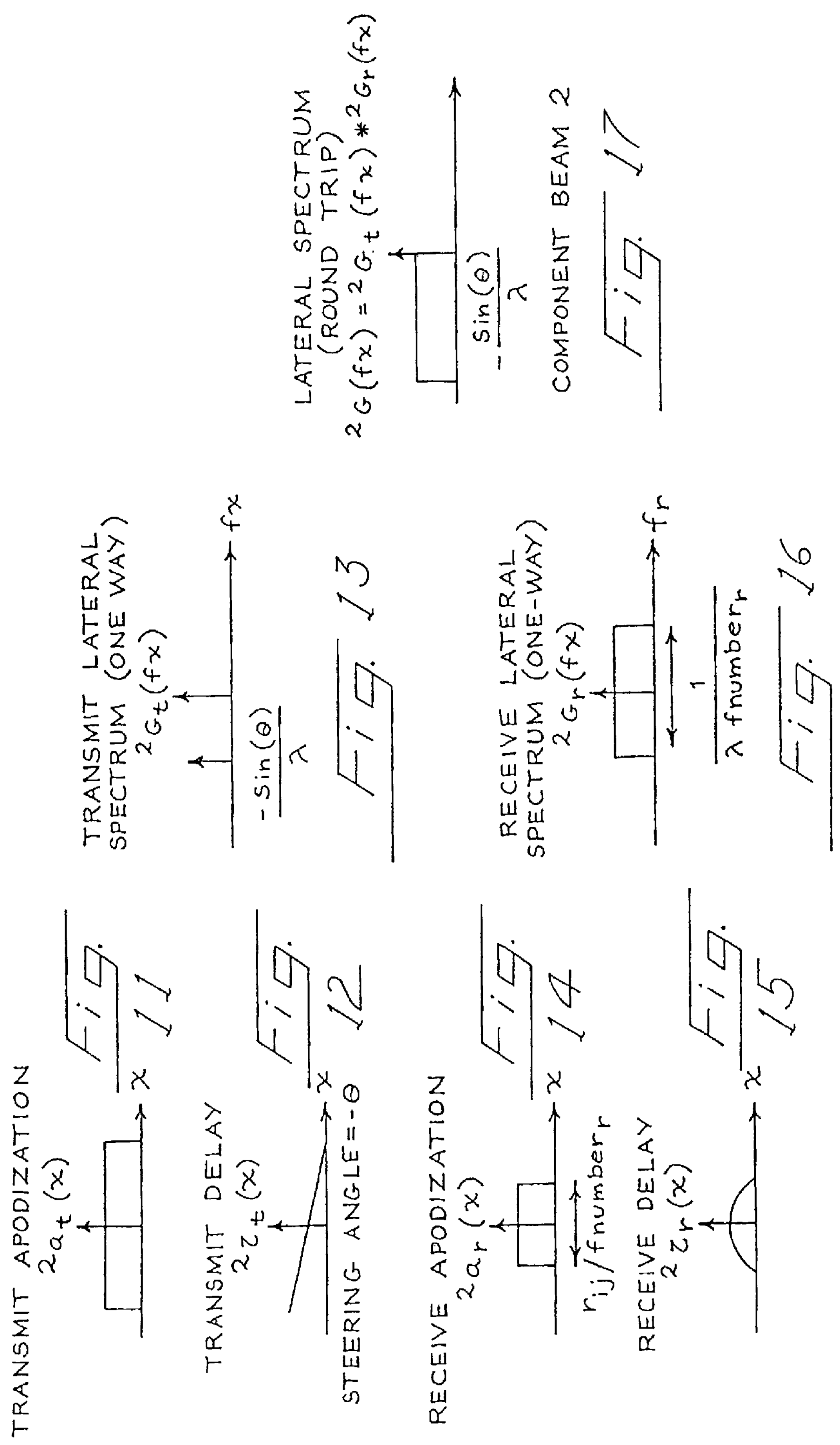

Fig. 11

Fig. 12

Fig. 13

Fig. 14

Fig. 15

Fig. 16

Fig. 17

LATERAL SPECTRUM
(SYNTHESIZED)

$$G(fx) = {}^{1}G(fx) + {}^{2}G(fx)$$

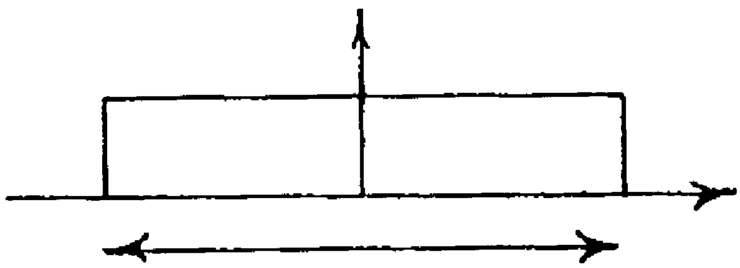

$$\frac{2}{\lambda\, fnumber_r}$$

SYNTHESIZED BEAM

Fig. 18

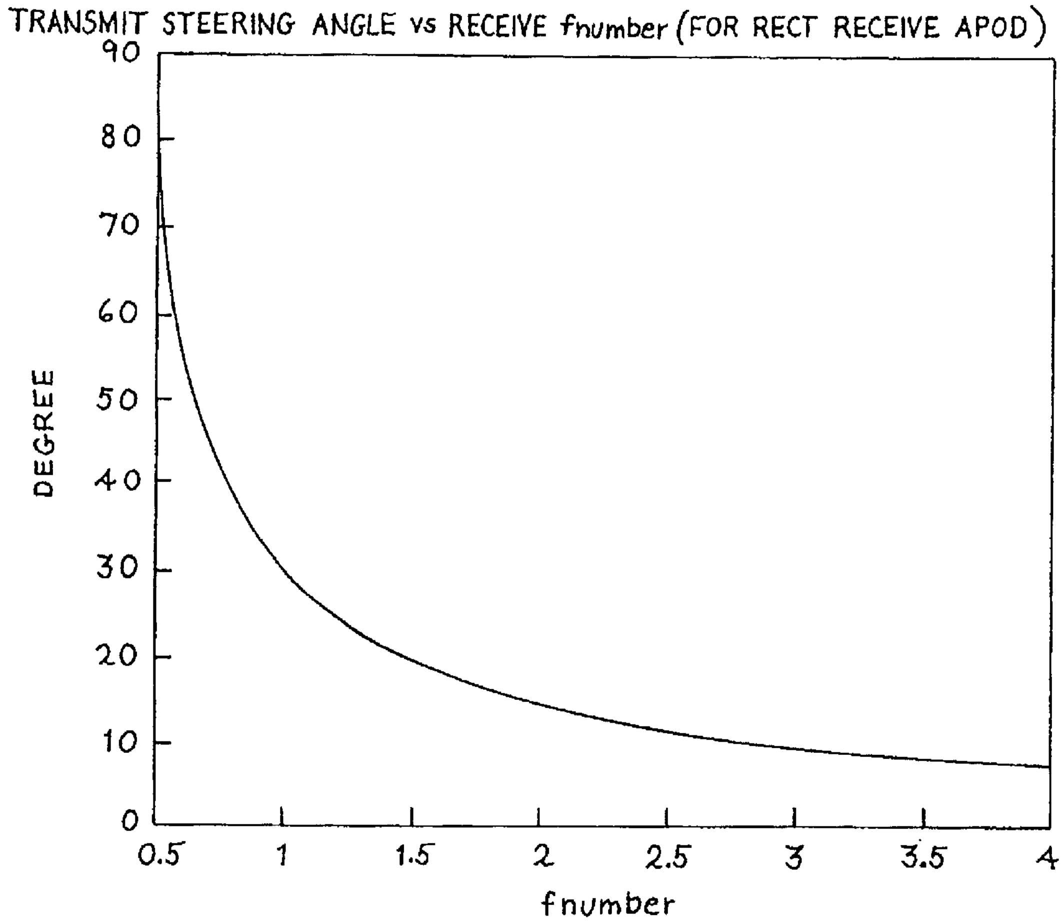

Fig. 19

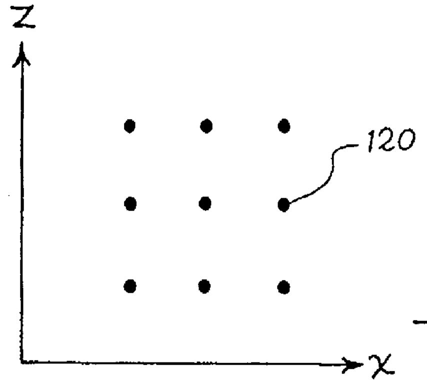

Fig. 56

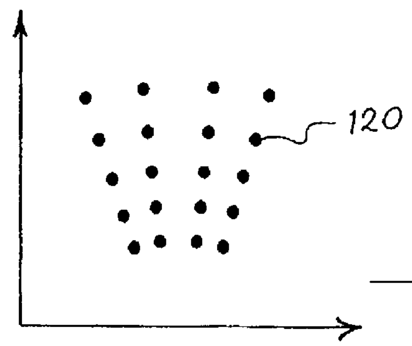

Fig. 57

PSF FOR RIGHT-STEERED Xmt PLANE WAVE, DYN RANGE = 60dB

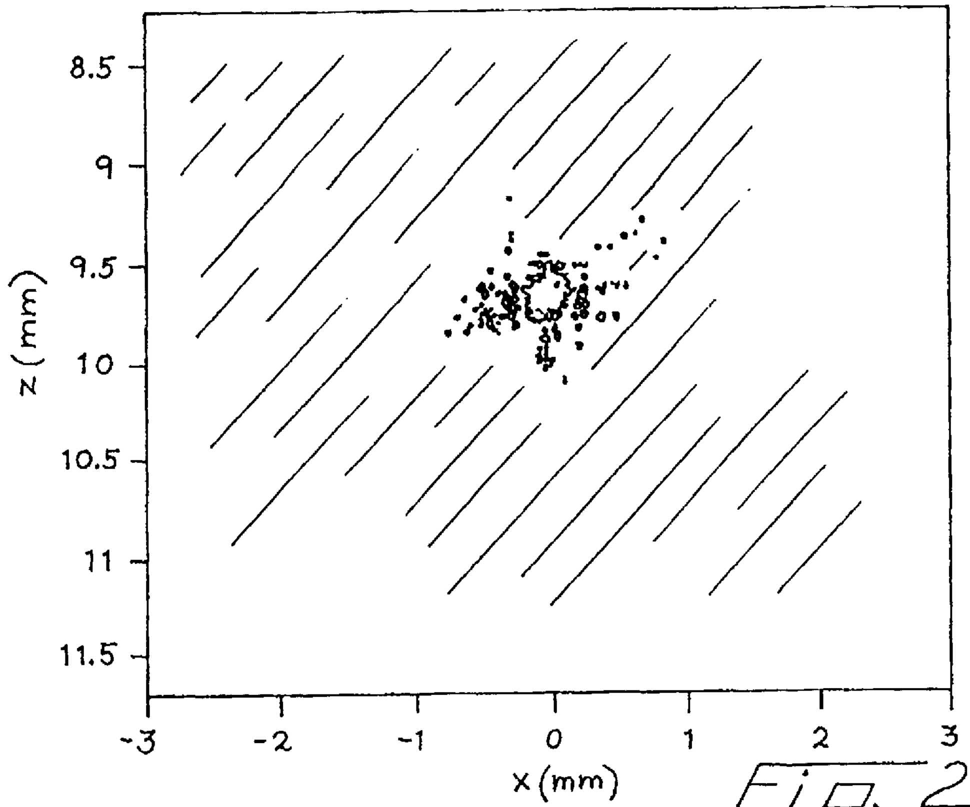

Fig. 20

PSF FOR LEFT-STEERED Xmt PLANE WAVE

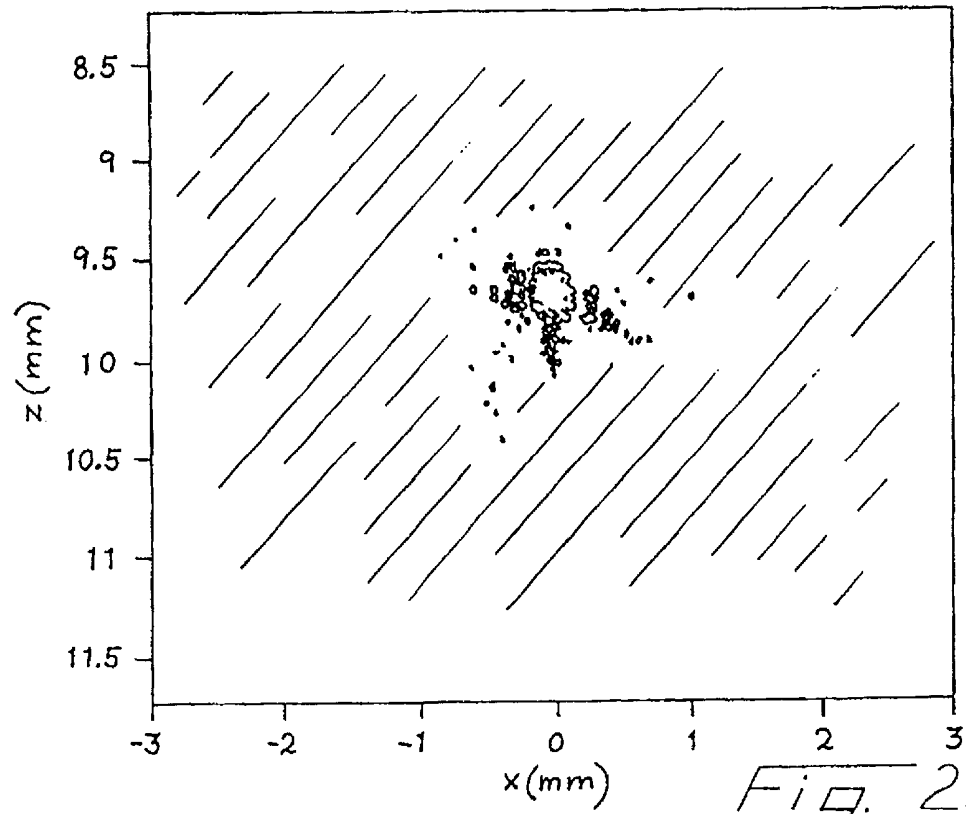

Fig. 21

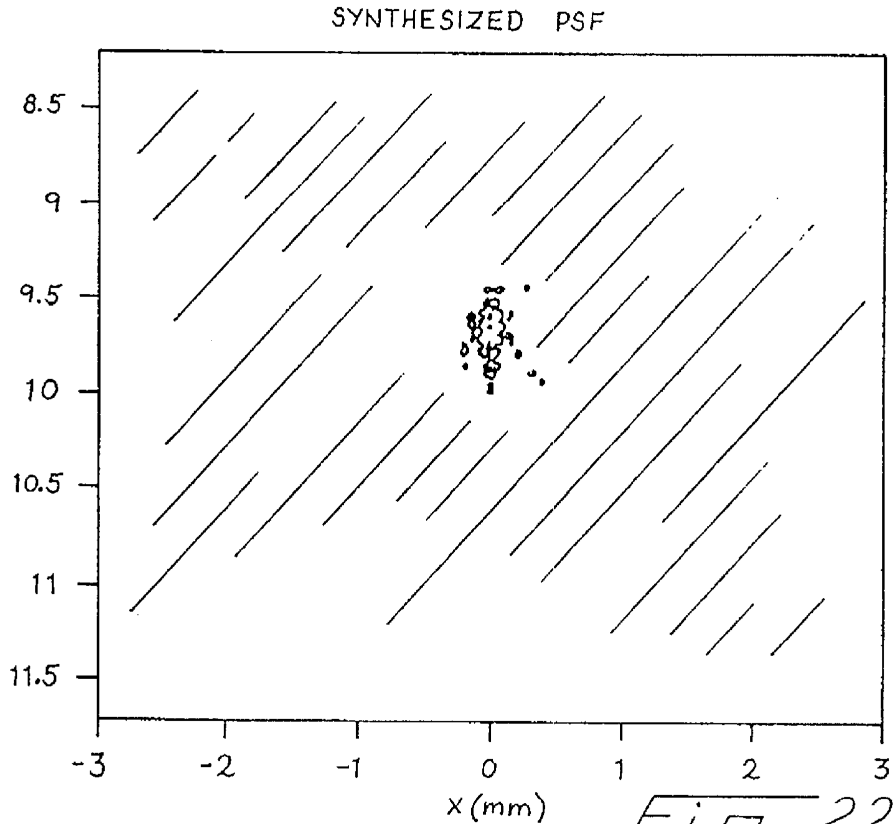
SYNTHESIZED PSF
8.5
9
9.5
10
10.5
11
11.5
z (mm)
-3
-2
-1
0
1
2
3
x (mm)

Fig. 22

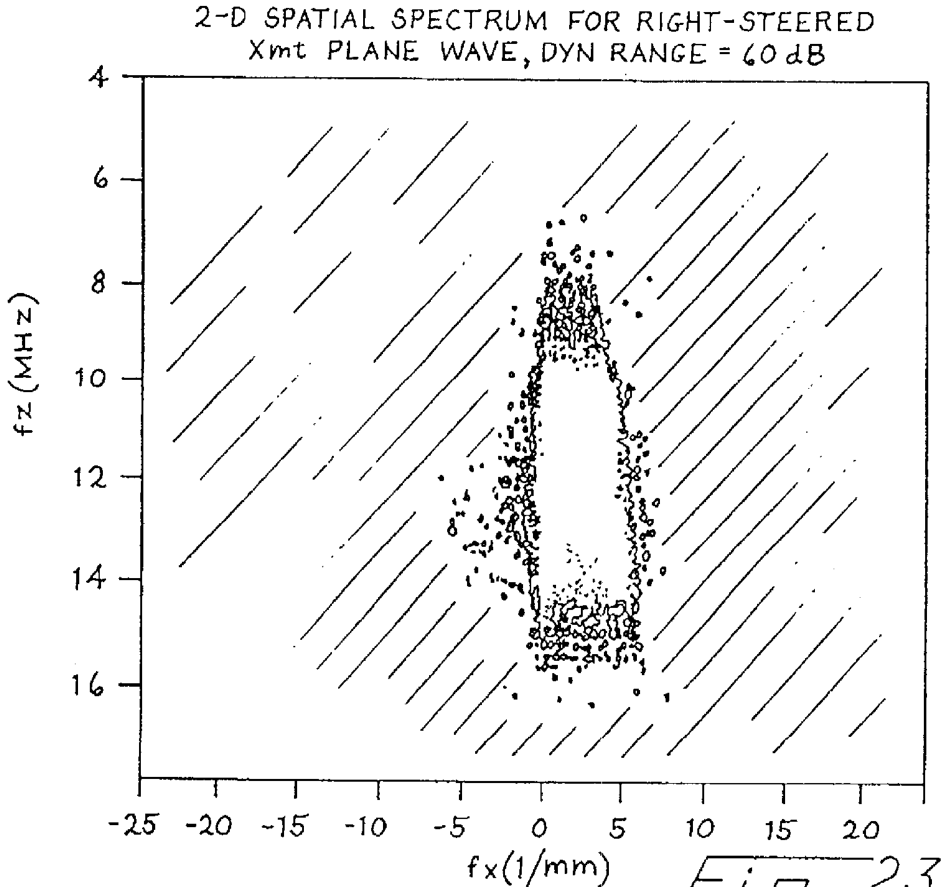
2-D SPATIAL SPECTRUM FOR RIGHT-STEERED
Xmt PLANE WAVE, DYN RANGE = 60 dB
4
6
8
10
12
14
16
fz (MHz)
-25
-20
-15
-10
-5
0
5
10
15
20
fx (1/mm)

Fig. 23

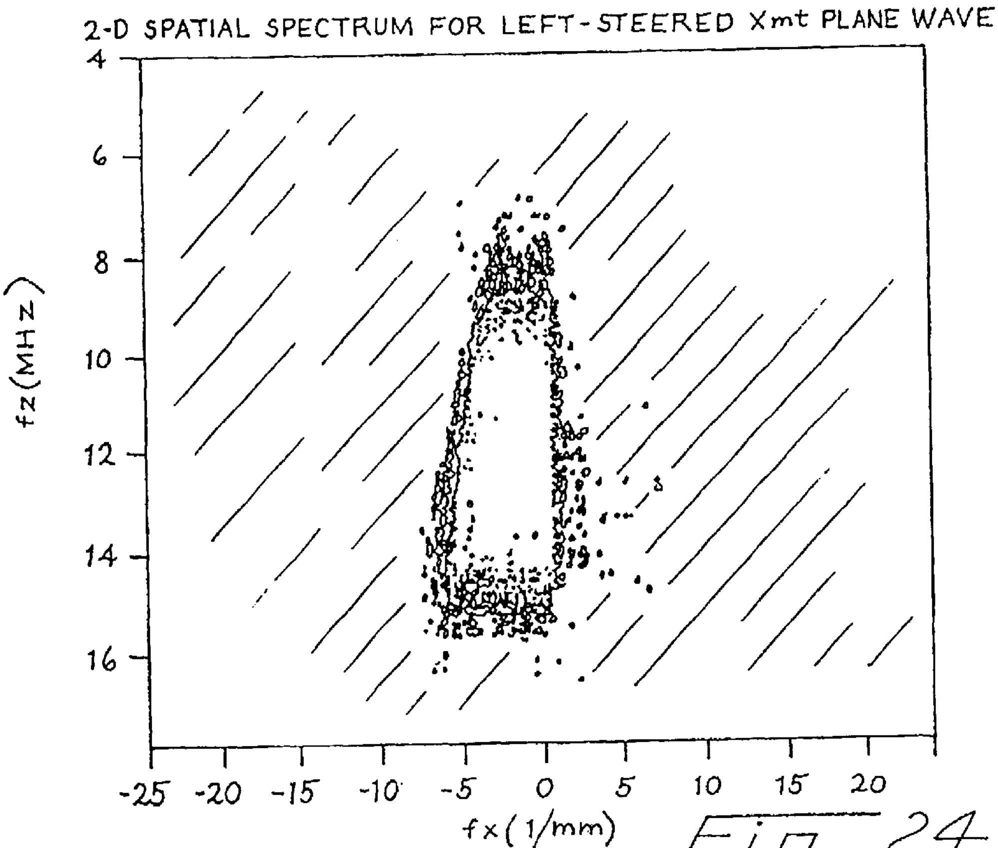
2-D SPATIAL SPECTRUM FOR LEFT-STEERED Xmt PLANE WAVE
fz(MHz)
4
6
8
10
12
14
16
-25 -20 -15 -10 -5 0 5 10 15 20
fx(1/mm)

Fig. 24

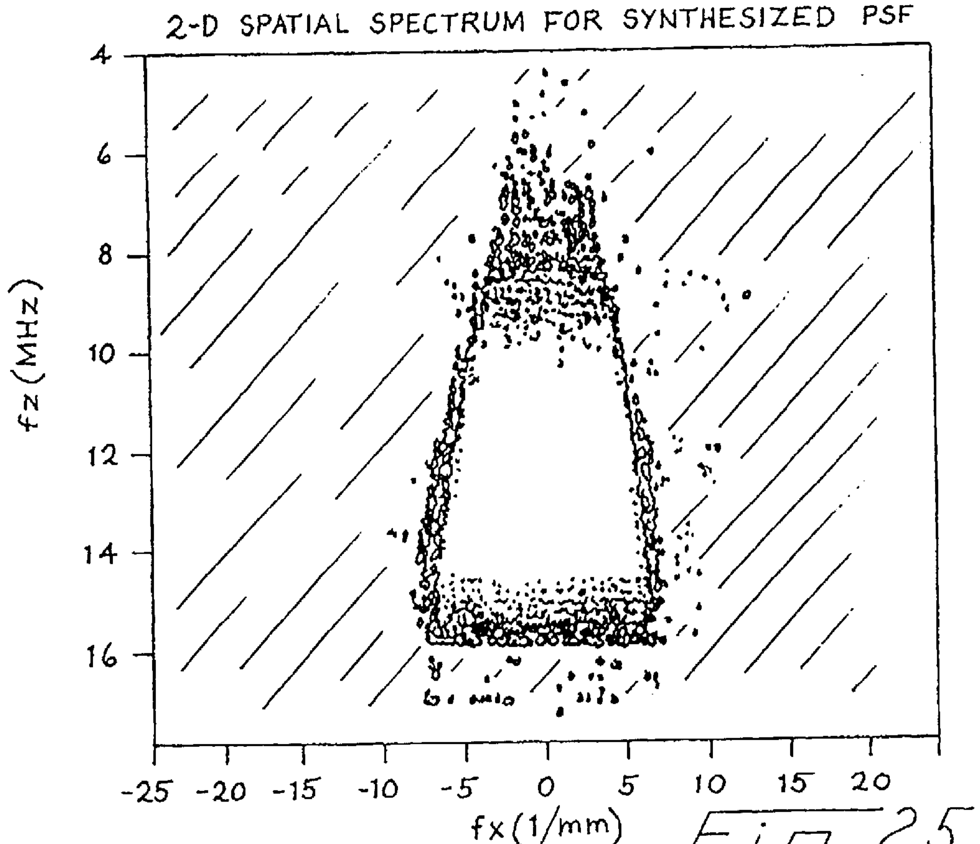
2-D SPATIAL SPECTRUM FOR SYNTHESIZED PSF
fz(MHz)
4
6
8
10
12
14
16
-25 -20 -15 -10 -5 0 5 10 15 20
fx(1/mm)

Fig. 25

Fig. 26

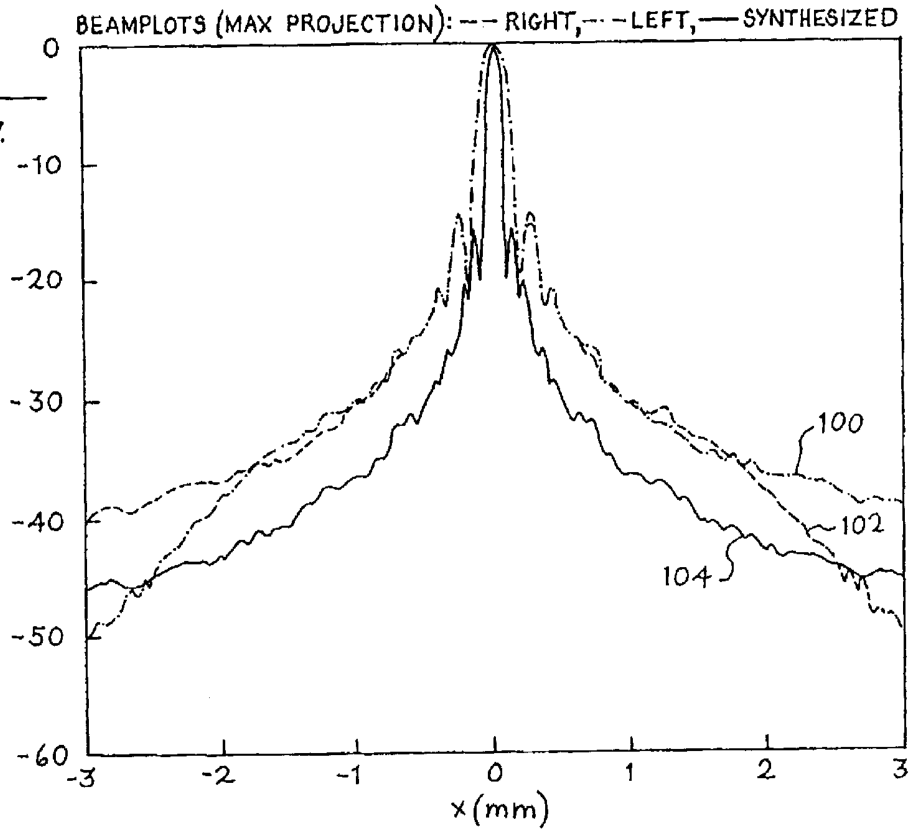
BEAMPLOTS (MAX PROJECTION): -- RIGHT, -·- LEFT, — SYNTHESIZED
0
-10
-20
-30
-40
-50
-60
-3
-2
-1
0
1
2
3
x (mm)
100
102
104

Fig. 27

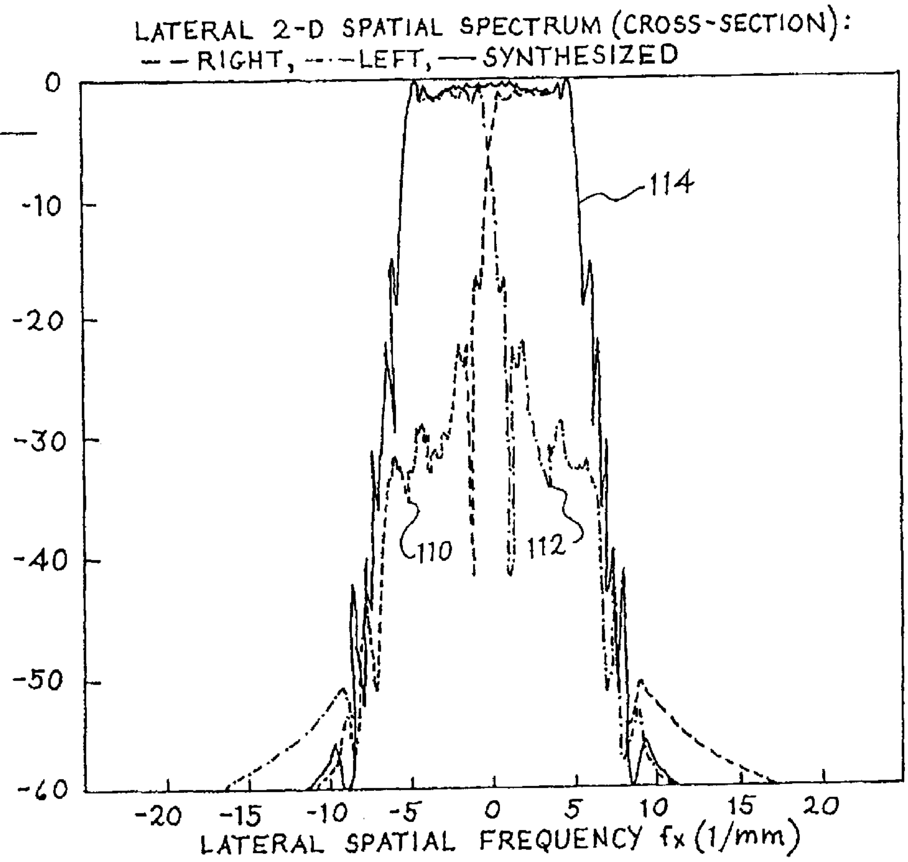
LATERAL 2-D SPATIAL SPECTRUM (CROSS-SECTION):
-- RIGHT, -·- LEFT, — SYNTHESIZED
0
-10
-20
-30
-40
-50
-60
-20
-15
-10
-5
0
5
10
15
20
LATERAL SPATIAL FREQUENCY fx (1/mm)
114
110
112

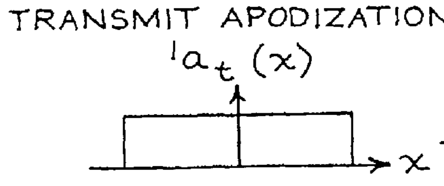

Fig. 28

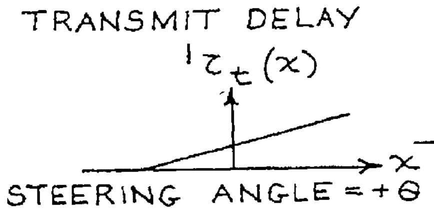

Fig. 29

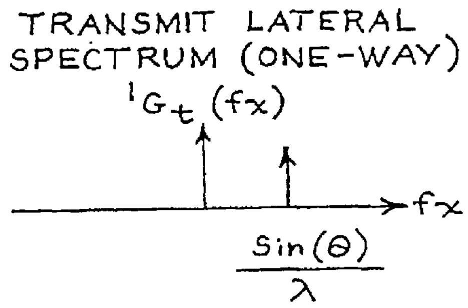

Fig. 30

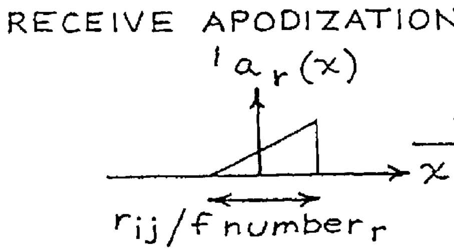

Fig. 31

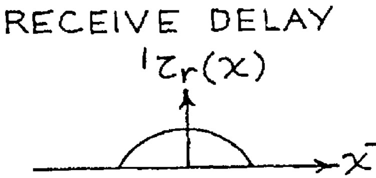

Fig. 32

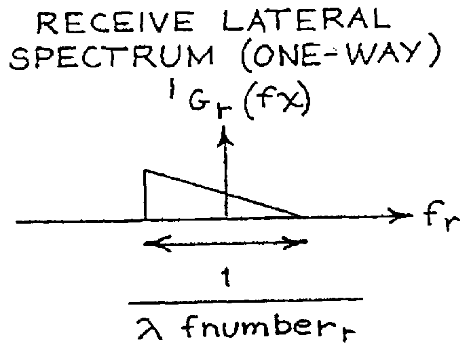

Fig. 33

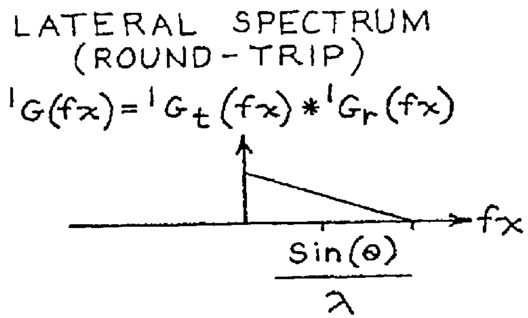

COMPONENT BEAM 1

Fig. 34

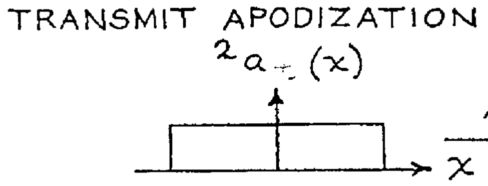

Fig. 35

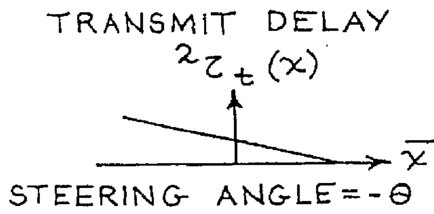

Fig. 36

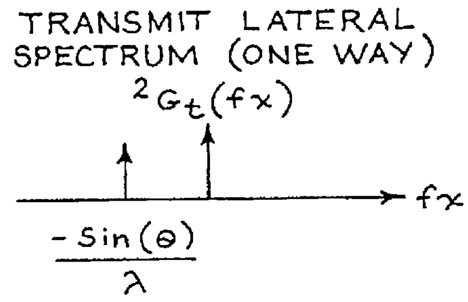

Fig. 37

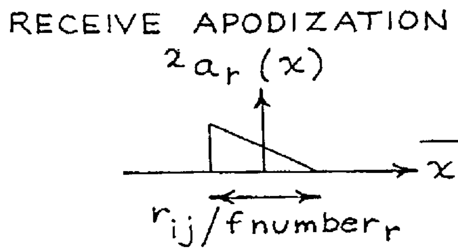

Fig. 38

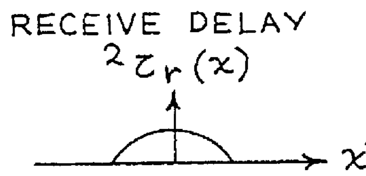

Fig. 39

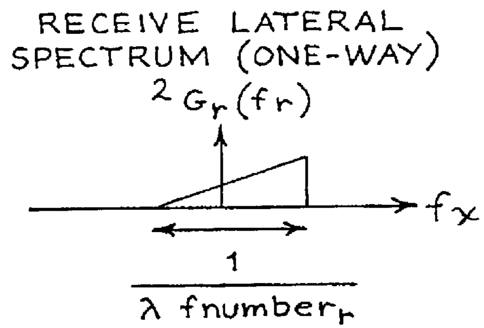

Fig. 40

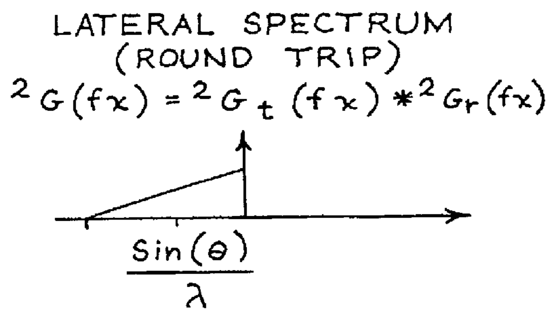

Fig. 41

LATERAL SPECTRUM
(SYNTHESIZED)

$$G(fx) = {}^{1}G(fx) + {}^{2}G(fx)$$

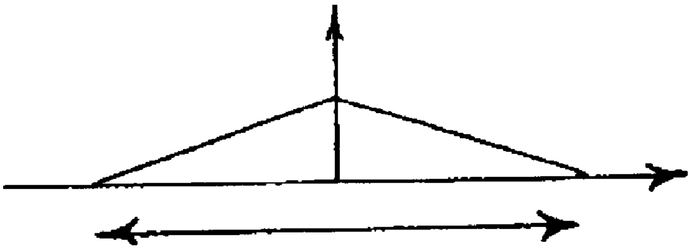

$$\frac{2}{\lambda \, fnumber_r}$$

SYNTHESIZED BEAM

Fig. 42

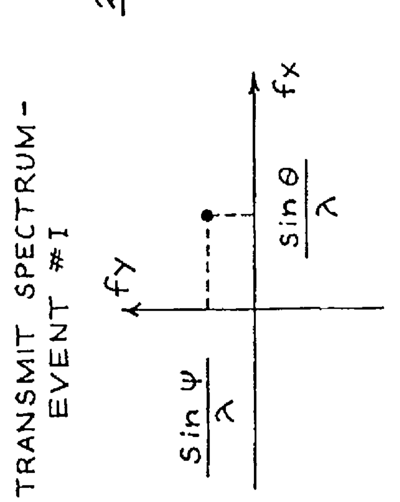

Fig. 43

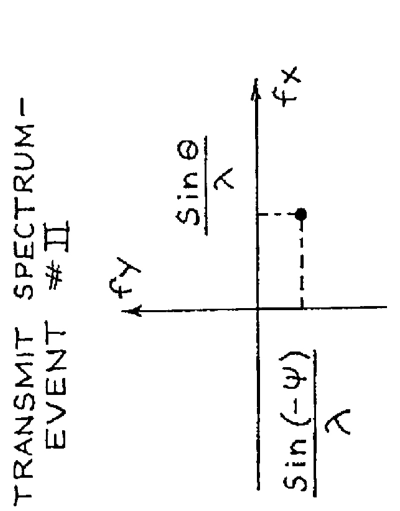

Fig. 44

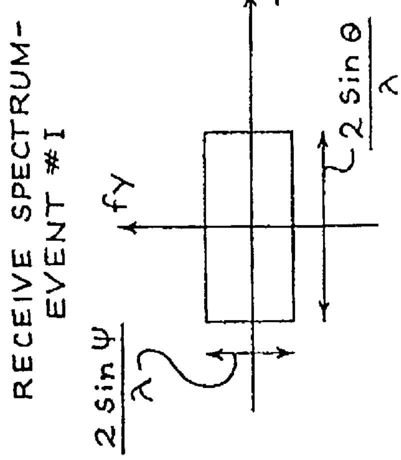

Fig. 47

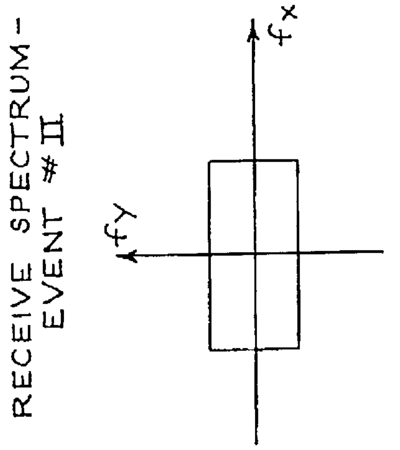

Fig. 48

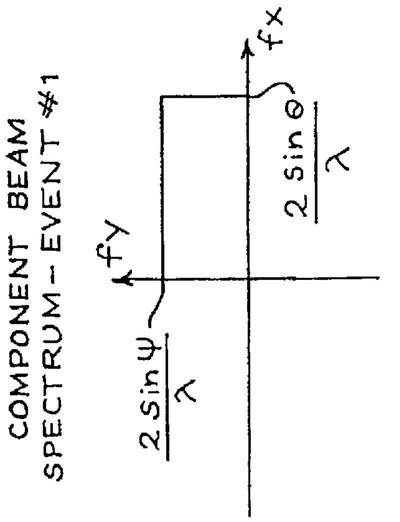

Fig. 51

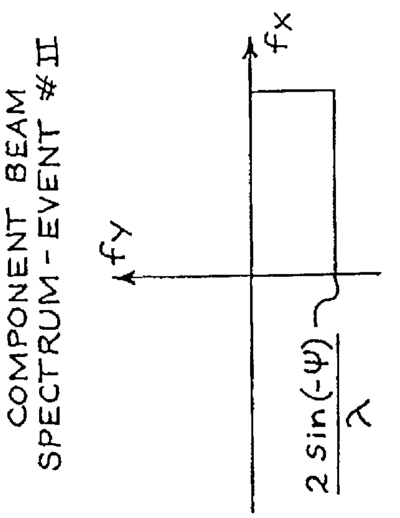

Fig. 52

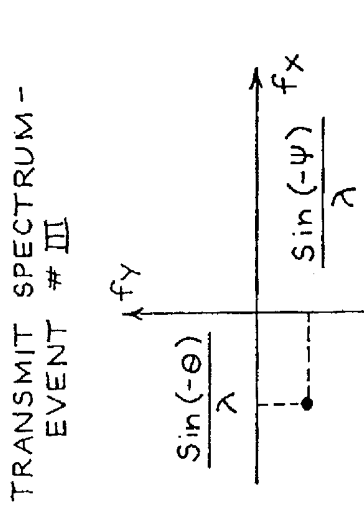

Fig. 45

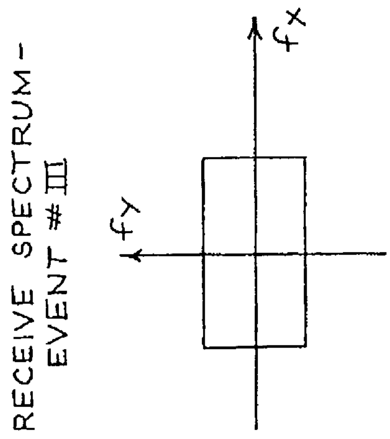

Fig. 49

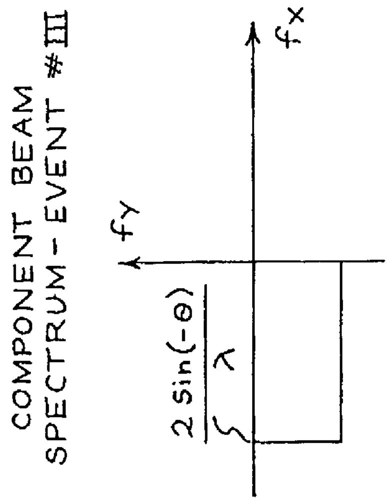

Fig. 53

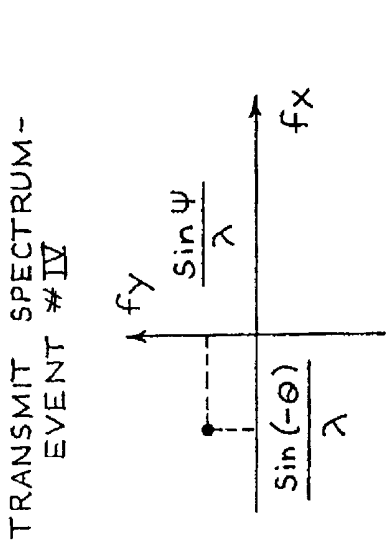

Fig. 46

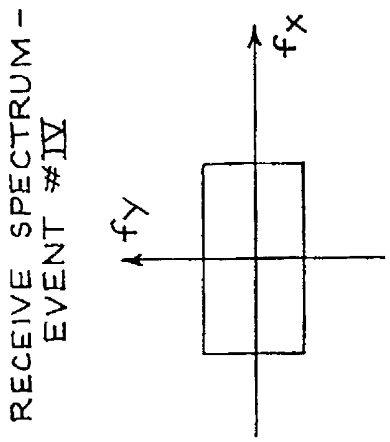

Fig. 50

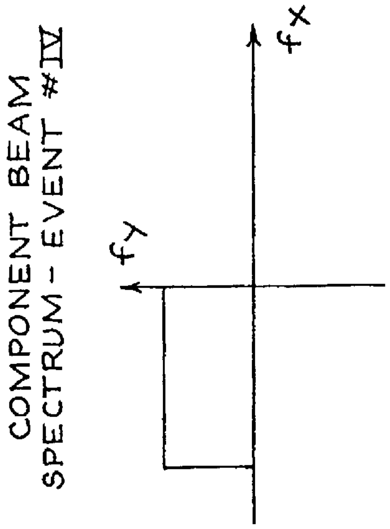

Fig. 54

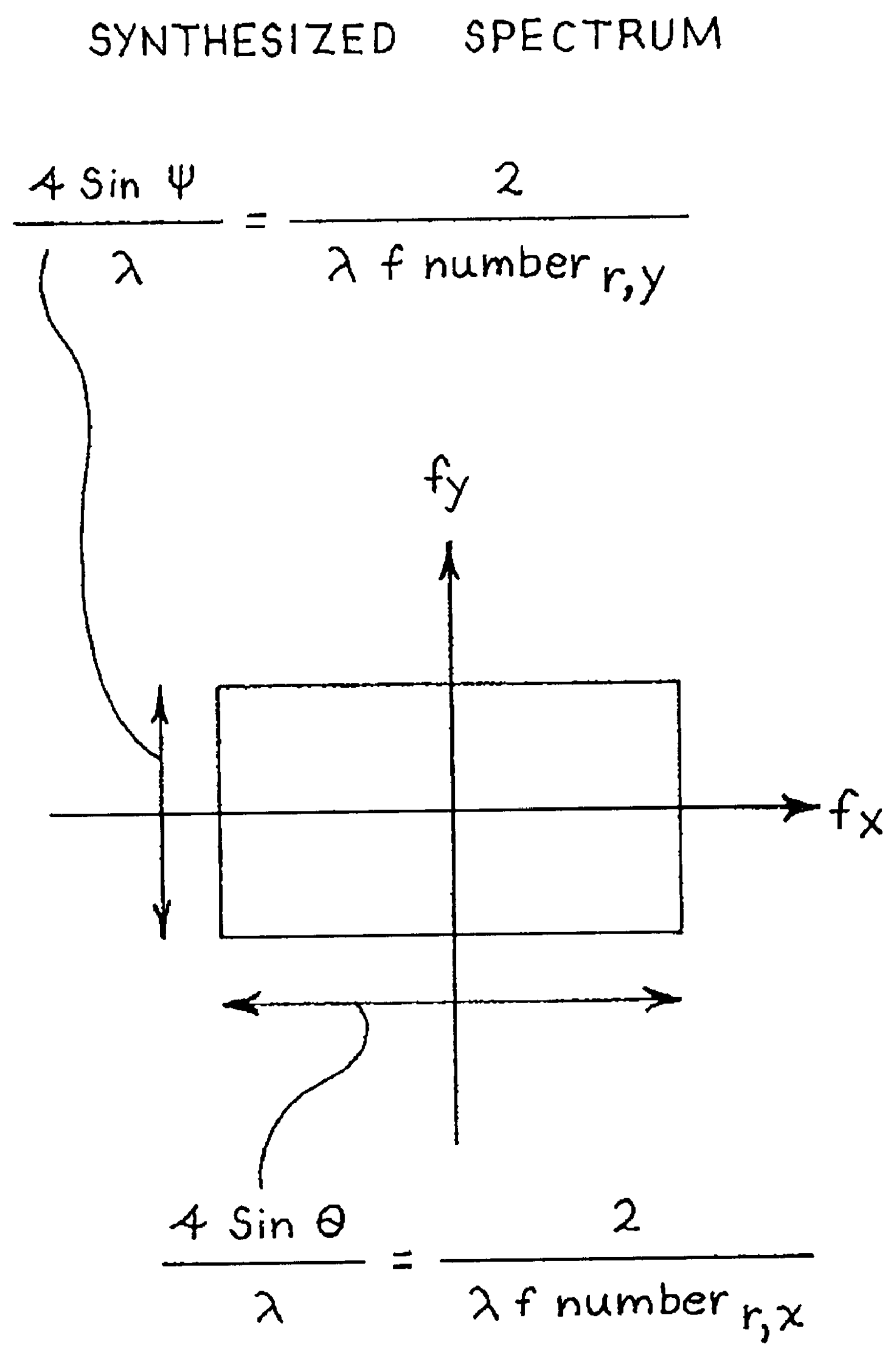
SYNTHESIZED SPECTRUM
$\frac{4 \sin \Psi}{\lambda} = \frac{2}{\lambda \, f\,number_{r,y}}$
f_y
f_x
$\frac{4 \sin \Theta}{\lambda} = \frac{2}{\lambda \, f\,number_{r,x}}$

Fig. 55

FIG. 58

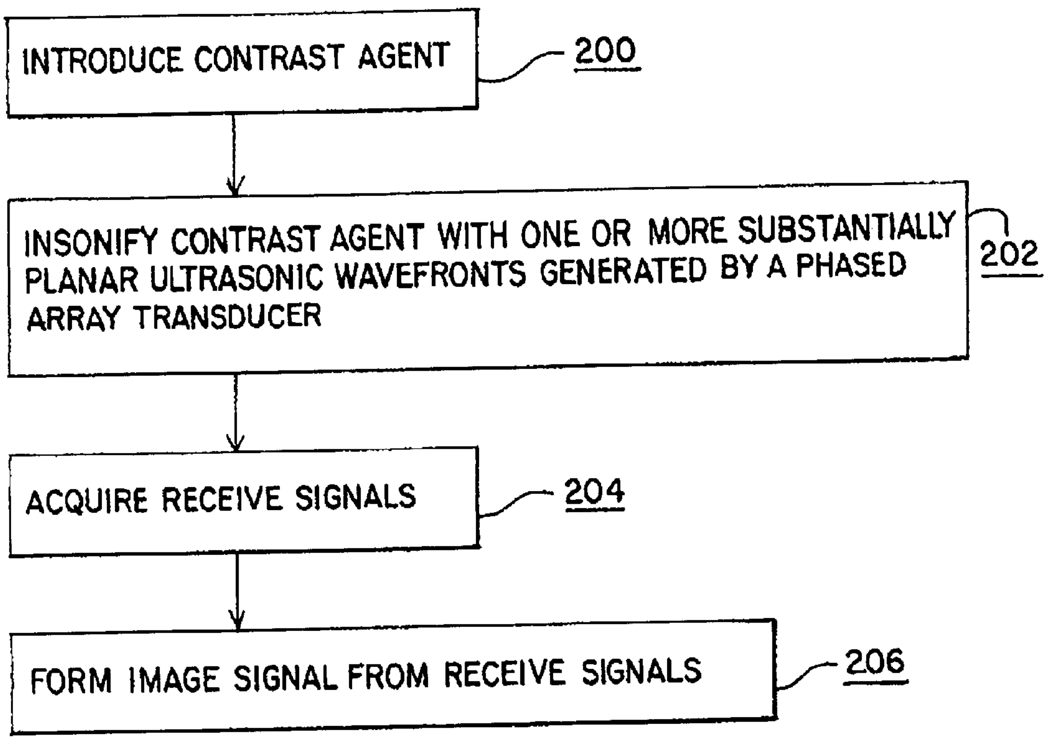
INTRODUCE CONTRAST AGENT
200
INSONIFY CONTRAST AGENT WITH ONE OR MORE SUBSTANTIALLY PLANAR ULTRASONIC WAVEFRONTS GENERATED BY A PHASED ARRAY TRANSDUCER
202
ACQUIRE RECEIVE SIGNALS
204
FORM IMAGE SIGNAL FROM RECEIVE SIGNALS
206

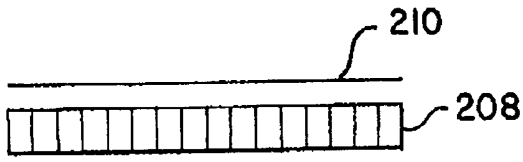

FIG.59a

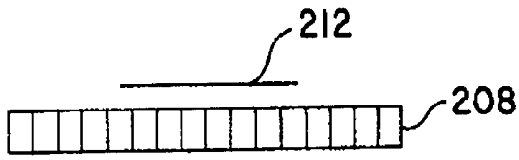

FIG.59b

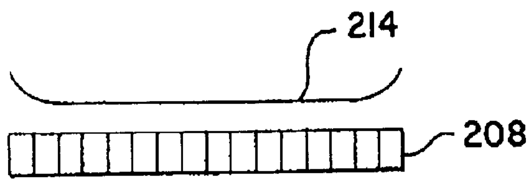

FIG.59c

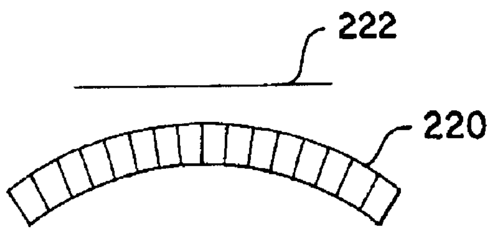

FIG.59d

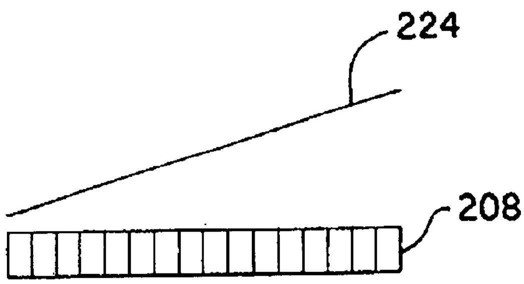

FIG.59e

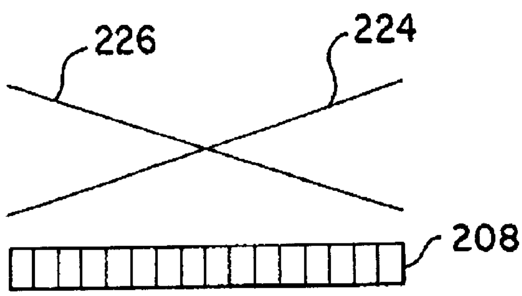

FIG.59f

FIG.59g

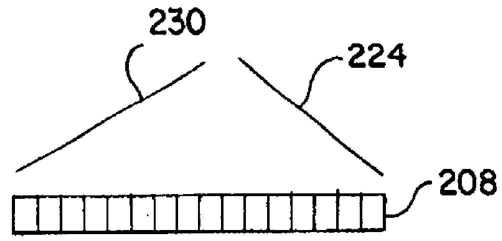

FIG.59h

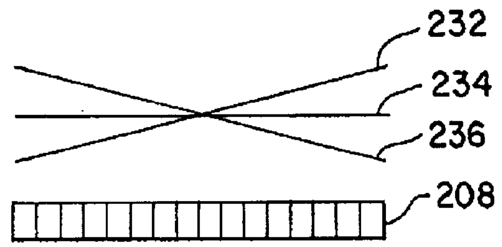

FIG.60

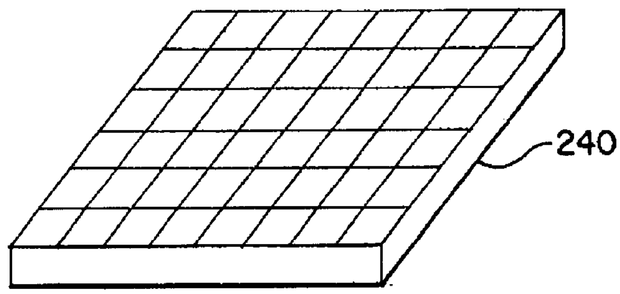

FIG.61

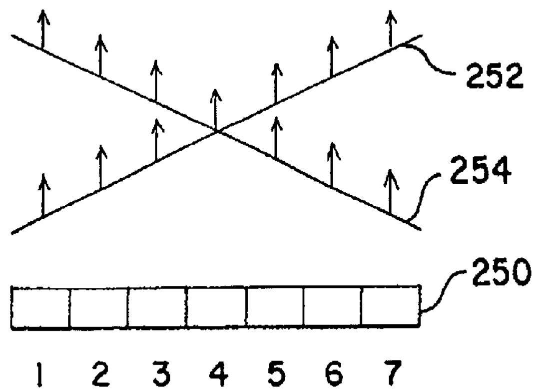

FIG. 62

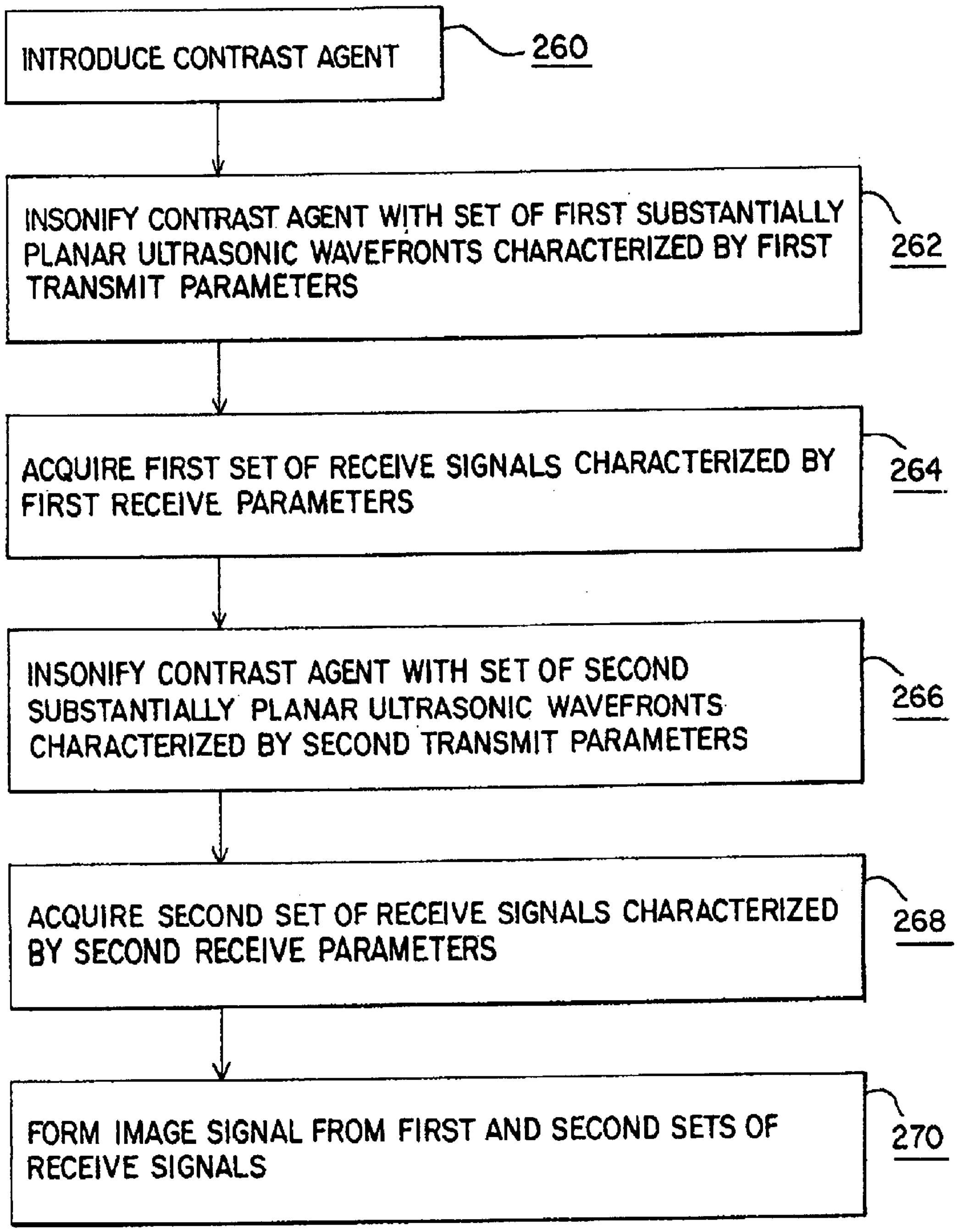
INTRODUCE CONTRAST AGENT
260
INSONIFY CONTRAST AGENT WITH SET OF FIRST SUBSTANTIALLY PLANAR ULTRASONIC WAVEFRONTS CHARACTERIZED BY FIRST TRANSMIT PARAMETERS
262
ACQUIRE FIRST SET OF RECEIVE SIGNALS CHARACTERIZED BY FIRST RECEIVE PARAMETERS
264
INSONIFY CONTRAST AGENT WITH SET OF SECOND SUBSTANTIALLY PLANAR ULTRASONIC WAVEFRONTS CHARACTERIZED BY SECOND TRANSMIT PARAMETERS
266
ACQUIRE SECOND SET OF RECEIVE SIGNALS CHARACTERIZED BY SECOND RECEIVE PARAMETERS
268
FORM IMAGE SIGNAL FROM FIRST AND SECOND SETS OF RECEIVE SIGNALS
270

METHOD AND APPARATUS FOR FORMING MEDICAL ULTRASOUND IMAGES

CROSS-REFERENCE TO RELATED APPLICATION

This application is a continuation-in-part of U.S. patent application Ser. No. 09/518,972, filed Mar. 16, 2000, now U.S. Pat. No. 6,309,356 the entirety of which is hereby incorporated by reference.

BACKGROUND

This invention relates to medical ultrasonic imaging, and in particular to methods for improving the imaging of contrast agents.

The nonlinear response of contrast agents is a unique property that improves the detectability of contrast agents in the blood and/or tissue. At the second harmonic, third harmonic, sub-harmonic, or other harmonics, the agents effectively generate signals that are unique to contrast agent. Since the contrast agent response to the incident sound wave is not linearly related to the impinging sound pressure, nonuniform peak pressure fields can generate nonuniform images of contrast agents that are much more nonuniform than corresponding tissue images at the fundamental frequency. Nonuniform images reduce diagnostic confidence. Even linear imaging of contrast agents or the combination of linear imaging with nonlinear imaging can produce nonuniform images due to inhomogeneous pressure fields.

For the detection and characterization of lesions in the liver and spleen, contrast agents such as Levovist are especially useful since they accumulate in healthy tissue to a greater extent than in diseased tissue. The imaging of these agents often shows dark voids where the lesions are detected, provided the peak pressure is sufficient to generate a strong nonlinear response from the contrast agent. With some imaging techniques, an agent such as Levovist generates a high-contrast image, where detected agent is shown much brighter than the surrounding contrast-free tissue or undetected (or poorly detected) agent. Nonuniform peak pressures in space can limit the area over which the contrast agents are detected, and low-brightness areas become suspicious areas and often need to be re-scanned.

Some contrast agents are preferably imaged using a low transmit peak pressure or low mechanical index (MI), since this reduces agent destruction, maintains agent concentration, and prolongs enhancement. Other contrast agents are preferentially detected by significant disruption or destruction with high transmit peak pressures. The conventional beamforming techniques (focussing transmitted pressure waves through time delays and phasing adjustments) produce nonuniform pressure fields as a function of depth. This reduces the area of good image enhancement at low as well as high transmit peak pressures.

SUMMARY

A technique that more uniformly distributes peak acoustic pressure over a given depth will increase the area over which contrast agents can be used to aid diagnosis. For some contrast agents and imaging situations, increasing the peak pressure above a pressure threshold may not produce noticeable increases in agent detectability. Techniques that can generate peak pressures above a threshold over a greater spatial extent, even with a possible reduction in maximum peak pressure in some areas, can produce improved images of contrast agents.

As described in detail below in conjunction with the preferred embodiments, the present inventors have discovered that transmitted plane waves, or wavefronts that are substantially planar can generate peak pressures that are more uniform over depth, and this improved uniformity can improve the detectability of contrast agents. Depending upon the type of contrast agent being used, the returned frequencies of interest (e.g., fundamental, harmonic, selected harmonic orders, or a combination of fundamental and one or more harmonic orders) and the desired strength of the nonlinear response, multiple substantially planar wavefronts can be generated at substantially the same time to increase peak pressures.

The foregoing remarks have been provided only by way of introduction, and they are not intended to narrow the scope of the following claims.

BRIEF DESCRIPTION OF THE DRAWINGS

FIG. **1** is a block diagram of a medical ultrasonic imaging system that incorporates a preferred embodiment of this invention.

FIGS. **2***a,* **2***b* and **2***c* are illustrations of regions R+, R– and R, respectively.

FIG. **(3)** is a block diagram of a method performed by the system of FIG. **1**.

FIGS. **4–18** are graphs illustrating respective steps of the method of FIG. **3** for a synthesized RECT-shape round-trip aperture function.

FIG. **19** is a graph showing a preferred transmit steering angle as a function of receive f-number (effective receive apodization shape of RECT is assumed).

FIGS. **20** and **21** show simulated point spread functions of the component beams for a right steered transmit plane wave and a left steered transmit plane wave, respectively.

FIG. **22** shows the point spread function of the beam synthesized by using the component beams shown in FIGS. **20** and **21**.

FIGS. **23**, **24** and **25** show the moduli of 2-D Fourier Transform (spatial spectra) for FIGS. **20**, **21** and **22**, respectively.

FIG. **26** shows the lateral responses, i.e., maximum projection beamplots, of the point spread function shown in FIGS. **20**, **21** and **22**.

FIG. **27** shows the lateral spectra, i.e., cross sections, of the 2-D spectra shown in FIGS. **23**, **24** and **25**.

FIGS. **28–42** are graphs illustrating respective steps of the method of FIG. **3** for a synthesized triangle-shaped round-trip aperture function.

FIGS. **43–55** are graphs illustrating steps of synthesizing a 2-D RECT-shaped spatial spectrum.

FIGS. **56** and **57** show two alternative distributions of image locations in a plane.

FIG. **58** is a block diagram of a method for imaging contrast agent with substantially planar ultrasonic wavefronts.

FIGS. **59***a*–**59***h* are schematic diagrams illustrating eight approaches to the generation of substantially planar ultrasonic wavefronts.

FIG. **60** is a schematic diagram of a two-dimensional transducer array suitable for generating substantially planar ultrasonic wavefronts.

FIG. **61** is a schematic diagram of a linear transducer array and two substantially planar ultrasonic wavefronts generated with this array.

FIG. **62** is a block diagram of another method for imaging contrast agent using substantially planar ultrasonic wavefronts.

DETAILED DESCRIPTION OF THE PRESENTLY PREFERRED EMBODIMENTS

Contrast Imaging with Substantially Planar Ultrasonic Wavefronts

Examples of beamformation techniques and methods that have been disclosed for imaging without contrast agents and that incorporate planar or nearly planar transmit wavefronts include the Sinc Waves [1, 2] and Xwaves using the Fourier Method [3]. The techniques of References [1] and [3] offer ways to increase frame rates, but compromises are made that degrade image quality. In some clinical situations these compromises may be unacceptable. When compared to the current standard of B-mode image quality, three significant compromises are reduced detail resolution, reduced contrast resolution, and/or loss in signal strength or signal-to-noise ratio (SNR). Axial detail resolution is compromised with Sinc Waves [1] due to the need for narrowband frequency responses (i.e., longer transmit pulses than conventionally used for B-mode imaging) to maintain good main lobe to side-lobe ratios and large depths-of-field. The contrast resolution of all these techniques can be degraded due to high side-lobes in the resulting two-way acoustic beam patterns. Further, signal-to-noise ratios can be degraded due to less sound reaching the target of interest due to the reduced focussing used on transmit as compared to conventional beamforming techniques.

Two unique characteristics of contrast agents minimize the effects of the above-mentioned compromises and enhance the detectability of agents when a clinician is interested in blood-filled spaces. By combining any technique that uses transmitted planar or near-planar waves with contrast agents, improved detectability of these blood-filled spaces is possible. Contrast agents offer increased reflectivity for both linear imaging and nonlinear imaging. Thus, the effective SNR is increased and planar wavefronts can be used to detect contrast agent. Contrast agents also offer wideband frequency responses with narrowband frequency excitation. When exciting some contrast agents with a transmitted pulse of x(t), the returned pulse can exhibit signals proportional to $x^n(t)$, where n is a number greater than one. These returned signals are shorter, or equivalently of broader bandwidth, and increased detail resolution. Also, the present inventors have learned that disrupted or destroyed contrast agents can exhibit bandwidths that are broader than the transmitted signals, thus further increasing axial resolution. Further, the present inventors have discovered that the generation of an image using a very broadband receive filter that includes signals at and near the fundamental and second harmonic frequencies can significantly increase the axial detail resolution. In some situations, the absence of any receive filter may be preferred. Therefore, the use of contrast agents with techniques that transmit planar or near-planar wavefronts will not suffer from poor axial resolution, even when narrowband transmit pulses are used.

Contrast agents also improve contrast resolution due to improved agent reflectivity. Since a contrast-filled lesion or vessel is more easily identified by its greater returned signal strength relative to the surrounding contrast-free tissue, contrast agents, as their name implies, increase contrast resolution. Further, when imaging with contrast agents the ability to reconstruct a target accurately in the image is of lesser importance as compared to the ability simply to detect the presence of a target such as contrast agent. Thus, high side-lobes next to an acoustic beam pattern's main lobe are less detrimental to image quality. High side-lobes in a non-contrast B-mode image can significantly reduce one's ability to see subtle changes in echogenicity, whereas high side-lobes in a contrast image will not significantly reduce one's ability to identify contrast agent.

The following general discussion will make reference to FIGS. **58–62**. Specific preferred systems for generating substantially planar wavefronts will then be described in conjunction with FIGS. **1–57**.

As shown in FIG. **58**, a medical ultrasonic imaging method for imaging contract agent begins in block **200** by introducing a contrast agent into the tissue of interest. As used herein, the term "contrast agent" is intended broadly to refer to liquids, suspensions, and fluids (including, for example, suspensions of microbubbles) that are introduced into a biological tissue to improve the contrast of the resulting image. Levovist is one example of a well-known contrast agent. Contrast agent can be introduced into the tissue in any suitable way, including by injection at a peripheral vein. This invention is not limited to any particular contrast agent, or to any particular method for introducing the contrast agent to the tissue.

Once the contrast agent has been introduced, it is insonified in block **202** with one or more substantially planar ultrasonic wavefronts generated by a phased array transducer. The following sections of this specification discuss alternative apparatus and methods that can be used to generate such substantially planar ultrasonic wavefronts. As used herein, the term "substantially planar" or "near-planar" as applied to a wavefront is defined as a pressure wavefront that leaves the transducer elements of the transducer within the active aperature, wherein at least 25% of the transmitted envelopes of the wavefront have substantially identical phases when programmed in the transmit beamformer. The term "substantially identical phases" includes phases within one wavelength of the center frequency of the average of the transmit pulses among the active transmit aperture. Here, the center frequency is defined as the first moment, or "center of mass", of the transmitted pulse spectra. Note, a "substantially planar" or "near planar" wavefront as programmed into a transmit beamformer may actually deviate from a substantially planar wavefront upon conversion to a pressure wavefront by the transducer due to several factors, but by the definition used here is still "substantially planar" or "near planar". These factors may include variations in sensitivity between different transducer elements, variations in the frequency response between elements, variations in the phase response between elements, linear or nonlinear variations in the electronics associated with different elements, tissue attenuation or abberations immediately in front of different elements, and the like.

Next, in block **204**, receive signals are acquired from echoes of the transmitted, substantially planar ultrasonic wavefronts, and in block **206** image signals are formed from the receive signals.

This invention is suitable for use with all forms of receive processing, including multiple-beam beamformers that generate more than one receive beam in response to a single transmit event. Conventionally, receive beamformers are dynamic, and they operate to focus the detected signals for more than one element at more than one location in space after a single transmit event. Receive processing can be adapted for any desired ultrasonic imaging mode, including for example B-mode imaging, Doppler imaging, and the like.

FIGS. **59*a*–59*h*** illustrate various alternative substantially planar ultrasonic wavefronts and the transducer arrays that produce them. As shown in FIG. **59***a,* a conventional one dimensional transducer array **208** includes multiple transducer elements. When suitable transmit signals are applied to these transducer elements, the result is a planar wavefront **210** that propagates away from the face of the transducer array **208**.

FIG. **59***b* illustrates a related mode of operation of the transducer array **208**, in which a smaller planar wavefront **212** is generated utilizing a smaller number of active transducer elements. The transmit waveform **212** is useful, for example, when minimizing unnecessary agent destruction or disruption in a case where a specific ultrasonic imaging system was unable to generate all desired receive beams over an area greater than the area covered by the propagating planar wavefront. Practical imaging systems will on occasion be limited by the memory used to store the receive signals from each transducer element and will have additional receive beamforming processing limitations. With current processing speeds and hardware limitations, it may be desirable to transmit a second planar wavefront slightly shifted relative to the previously transmitted planar wavefront, and to process a set of receive beams that covers the new area. This approach, which generates an image from more than one transmit event, can also minimize artifacts generated from movement during scanning that may occur during the time it takes to process many receive beams.

FIG. **59***c* illustrates the use of the transducer array **208** to form a substantially planar wavefront **214** that includes some focusing at the ends of the array **208** to improve peak signal energy at greater depths. This approach can be used to maintain peak pressure levels when tissue attenuation weakens returned signals.

FIG. **59***d* illustrates a differently shaped transducer array **220** that is in this example a curved array. As known to those skilled in the art, a curved array **220** can be used to generate a planar or a near-planar wavefront **222** by properly selecting the timing of transmit signals applied to individual transducer elements.

FIG. **59***e* illustrates the use of the transducer array **208** to create a steered planar wavefront **224** having a steering angle that forms an acute angle with the face of the transducer array **208**.

FIG. **59***f* illustrates use of the transducer array **208** to transmit two separate planar wavefronts **224**, **226** that are transmitted at different steering angles during the same transmit event. In this case, both wavefronts **224**, **226** are travelling within the tissue at the same time. This approach can be used to increase peak pressures along a desired direction and to excite or disrupt contrast agent in the tissue. Multiple dynamically-received beams can be focused along the direction of intersection and in parallel to the direction of intersection but still near the main direction of propagation.

FIG. **59***g* illustrates use of the transducer array **208** to form two steered planar wavefronts **228**, **230** that do not overlap in transducer element number. This approach can increase the area of detection as compared to the approach of FIG. **59***f* if an intersection of two or more plane waves is not necessary to generate sufficient peak pressures.

FIG. **59***h* illustrates use of the transducer array **208** to form three planar wavefronts **232**, **234**, **236** that are transmitted during the same transmit event. This example illustrates that many planar wavefronts can be transmitted during the same transmit event. This use of many planar wavefronts is similar to (and can be implemented as described in) References [1] and [2] with the following difference: In the cited references there is a need to use many planar wavefronts to preferentially keep the side lobe levels small. If only a few planar wavefronts are used, the weak focusing that is obtained does not contribute to a large main lobe relative to the side lobes. However, for use in imaging contrast agents, as explained above, high level side lobes relative to the main lobe are less detrimental to acceptable image quality when the main goal is to detect the contrast agent rather than to reconstruct the target with high accuracy. Further, side lobe levels may be of insufficient pressure to detect contract agents near the acoustic beam's main lobe.

FIG. **60** illustrates a two-dimensional array **240** that can be used to generate the planar and substantially planar wavefronts described above. In general, a transducer array that includes more than a single row of transducer elements can be implemented as a 1.25-, 1.5-, 1.75-, or a 2-dimensional transducer array, all of which are suitable for use with this invention.

Practical imaging systems provide finite transmit voltages for generating transmit waveforms. A preferred approach for configuring transmit events that contain more than one planar wavefront is to maintain the maximum transmit voltage on as many of the transducer elements as possible. For example, when a transducer array **250** is used to generate two simultaneous planar wavefronts **252**, **254**, as shown in FIG. **61**, one element would ideally be excited with twice the voltage as that used to excite the other elements. For those applications that demand maximum pressure, one approach is to maintain the maximum transmit voltage on all elements. Thus, in the example of FIG. **61**, element **4** is excited with the same maximum voltage as that used on the remaining elements **1**, **2**, **3**, **5**, **6**, and **7**. In FIG. **61** an arrow indicates the center of the envelope of each transmit waveform.

For those applications that do not demand maximum transmit pressure (e.g. low transmit power second harmonic imaging with contrast agents), the compromise discussed above may not be necessary, and the superposition of two or more planar or near-planar wavefronts is straightforward.

FIG. **62** provides a flow chart of another method for imaging contrast agent. Blocks **260**, **262**, and **264** are substantially similar to blocks **200**–**204** described above. The method of FIG. **62** differs from that of FIG. **58** in that contrast agent is insonified with a second set of substantially planar ultrasonic wavefronts characterized by second transmit parameters in block **266**, and then a second set of receive signals characterized by second receive parameters is acquired in block **268**. The image signal is formed from both the first and second sets of receive signals in block **270**.

Thus, a wide variety of transmit parameters can be varied between the two sets of substantially planar ultrasonic wavefronts, including envelope modulation frequency, envelope amplitude, envelope amplitude profile, envelope phase, and envelope phase profile. Similarly, a wide variety of receive parameters can be varied between the first and second sets of wavefronts, including apodization function, demodulation frequency, envelope amplitude, envelope amplitude profile, envelope phase, and envelope phase profile. Coded transmit pulses, such as chirped excitation pulses, may be used on a subset of elements for a single planar wavefront or applied selectively among multiple transmit events.

This invention can be incorporated into the conventional signal processing path utilized for color flow imaging. Images showing detected contrast agent can be superimposed on the conventional B-mode images and shown in greyscale or color. The invention can also be incorporated into the conventional B-mode signal processing path. The generated images can be processed separately and superimposed with one or more second B-mode images. This allows different processing steps to be applied to the contrast image and the background image. It may be preferred not to use planar or near-planar wavefronts for the background B-mode image. Of course, planar or near-planar wavefronts may be used to generate only a single image, one that contains a reference or background B-mode image and areas where contrast agent has been detected.

Planar or near-planar transmitted wavefronts can be used with single- or multiple-pulse imaging techniques. An example of a single-pulse technique is a second harmonic imaging technique that maintains second harmonic signals while suppressing fundamental signals through filtering. An example of a multiple-pulse technique is the use of conventional Doppler processing with multiple pulses of identical transmit characteristics. A preferred processing technique uses a first difference or second difference clutter filter, well known in the art. This preferred technique detects differences between receive pulses in a multiple-pulse sequence as an aid to the identification of contrast agents. Other techniques can also be used with the invention and include those described in U.S. Pat. No. 5,951,478 (Hwang), U.S. Pat. No. 5,632,277 (Chapman), and U.S. Pat. No. 6,095,980 (Burns), as well as in U.S. patent application Ser. No. 09/514,803.

A particular benefit associated with the detection of contrast agents with the beamformation techniques discussed hereafter is the less restrictive constraint on the receive beamformation process. Therefore, this invention is not limited to the techniques disclosed in the following sections of this specification.

As discussed below, it is desirable to maintain a smooth final spatial spectrum when two or more sub-spectra from component beams are combined. Any notches or spikes in the spatial spectra can produce undesirable acoustic beam patterns and objectionable target image reconstructions. For the detection of contrast agents, the sensitivity to the agent, or the ability to detect the agent, is often much more important than reconstructing the target structure with a high level of accuracy. Therefore, although smoothly varying spatial spectra are preferred, spectral spikes and notches are more tolerable when imaging contrast agents.

As explained above, the widest variety of imaging techniques can be used to transmit the planar and substantially planar wavefronts described above and to receive and process the resulting echoes. The following section of this specification describes particularly preferred methods for transmitting substantially planar ultrasonic wavefronts, and for receiving and processing these wavefronts.

Specific Embodiments

Turning now to the drawings, FIG. **1** shows a block diagram of a medical ultrasonic imaging system **10** that incorporates a preferred embodiment of this invention.

The system **10** includes a transmitter **12** that is coupled via a transmit/receive switch **14** to a transducer array **16**. The transmitter **12** applies transmit signals to the individual transducers of the array **16**, and these transmit signals are timed and phased to cause the array **16** to generate unfocused or weakly focused ultrasonic waves that insonify the region R from substantially different angles. In the following, for demonstration purposes, we will use planar arrays and a pair of plane waves steered at angles $\theta_1=+\theta$ and $\theta_2=-\theta$.

A wide variety of techniques can be used to implement the transmitter **12**, including both analog and digital techniques. The following U.S. patents, all assigned to the assignee of the present invention, provide examples of the types of approaches that can be used to implement the transmitter **12**: U.S. Pat. Nos. 4,550,607; 4,699,009; 5,148,810; 5,608,690; 5,675,554. These examples are, of course, not intended to be limiting in any way.

Similarly, the transducer array **16** can take any desired form. The transducer array **16** can be a 1-, 1.25-, 1.5-, 1.75-, two- or three-dimensional array. By way of example, the transducers described in any of the following of patents (all assigned to the assignee of the present invention) can readily be adapted for use with this invention: U.S. Pat. Nos. 5,261,408; 5,297,533; 5,410,208; 5,415,175; 5,438,998; 5,562,096; 5,657,295; 5,671,746; 5,706,820; 5,757,727; 5,792,058; 5,916,169; 5,920,523. Once again, this list is not intended to be limiting, and any suitable transducer array can be used.

Echo signals from the insonified regions R_+ and R_- (FIGS. **2***a* and **2***b*, respectively) are received by the transducer array **16** and are passed via the transmit/receive switch **14** to one or more AND converters **18**. The AND converters **18** digitize the receive signals formed by the transducer elements. In this example, the array **16** includes N separate transducer elements, and the system includes N separate A/D converters **18**.

The digitized receive signals are applied in parallel to one of several memories **20**, **22**. In this example, the memory **20** is used to store receive signals acquired in response to transmitted planar ultrasonic waves steered at a steering angle of $+\theta$, and the memory **22** is used to store receive signals acquired in response to transmitted planar ultrasonic waves steered at a steering angle of $-\theta$.

The memories **20**,**22** can be implemented as separate memory units, one for each transmit steering angle used, or they can alternately be implemented by a single memory unit that operates in a time-shared manner to store the receive signals associated with multiple transmit events. In alternative examples, more than two steering angles can be used, and it will often be convenient in such a case to provide more than two memories **20**, **22**. The memories **20**, **22** can be implemented as physically separate memories, or alternately they can be implemented as selected locations in a common physical device.

The system **10** also includes a plurality of beamformers **24**, **26**. The beamformers **24**, **26** form a multiplicity of beams from a single set of first receive signals stored in the memory **20** and a single set of second receive signals stored in the memory **22**, respectively. As one example, the beamformer **24** can form beams for M separate image locations from a single set of receive signals stored in the memory **20**, and the beamformer **26** can form beams for the same M image locations from a single set of receive signals stored in the memory **22**. Each of the beamformers **24**, **26** applies a selected apodization function and a selected time delay profile appropriate for the image location of interest, and then sums the apodized, delayed receive signals over the receive channels for each image location in the region of interest.

The beamformers **24**, **26** can be implemented as separate beamformers, or they can alternately be implemented by a single device that operates in a time-shared manner to form the desired beams. The beamformers **24**, **26** can be implemented using any suitable technology. For example, the beamformers described in the following U.S. patents (all assigned to the assignee of the present invention) can readily be adapted for use with this invention: U.S. Pat. Nos. 4,550,607, 4,699,009, and 5,555,534. As before, this list is not intended to be limiting.

Prior to amplitude detection, the beams thus formed are applied in parallel to a synthesizer **28** that forms synthesized beams for the overlap region R (FIG. 2*c*). The synthesizer **28** can form these synthesized beams as a coherent or partially coherent weighted sum of the first and second beams generated by the beamformers **24, 26**, respectively. The weights, in general, can be complex numbers with amplitude and phase. The synthesis function, in general, is a multi-input multi-output nonlinear function (mapping). This function can also be an adaptive one, adaptive to parameters derived from the input signals such as SNR, coherence factor, etc. This block may also include lateral and axial predetection filters.

The synthesized beams generated by the synthesizer **28** are applied to an amplitude detector **30**. Additional memory blocks (not shown in FIG. **1**) can be provided between the beamformers and the synthesizer and the synthesizer and the amplitude detector to store, respectively, the beamformed and synthesized images for further processing. The detected signals generated by the detector **30** are applied to an image processor **32** and then displayed on a display **34**. As before, the widest variety of detectors, image processors and displays can be adapted for use with this invention.

FIG. **3** provides a flow chart of a method implemented by the system **10** of FIG. **1** using planar waves. FIGS. **4–18** demonstrate how a RECT-shaped round-trip lateral frequency response with bandwidth $2/(\lambda\ \text{fnumber}_r)$ (twice the one-way bandwidth) is synthesized using the flow chart of FIG. **3**. To simplify the demonstration the continuous wave case will be considered first.

In block **50** of FIG. **3**, the system **10** of FIG. **1** transmits a first substantially planar wave at a steering angle of $\theta_1=+\theta$. FIGS. **4** and **5** respectively show the transmit apodization ${}^1a_t(x)$ and delay ${}^1\tau_t(x)$ profiles. The transmit apodization function is substantially constant, and utilizes all available transducer elements. The transmit delay profile increases linearly from one end of the transducer array to the other. If we temporarily ignore the effect of the finite spatial extent of the aperture, then at a spatial position (x_i,z_j) and time t, a plane wave steered at angle θ can be expressed by:

$$s(t,x_i,z_j,f)=e^{j\cdot 2\cdot\pi\cdot(f\cdot t-f_x\cdot x_j-f_z\cdot z_j)} \quad \text{(Eq. 1)}$$

where, f is the temporal CW excitation frequency, f_x is the lateral spatial frequency, $f_x=f\sin(\theta)/c=\sin(\theta)/\lambda$, f_z is the axial spatial frequency, $f_z=f\cos(\theta)/c=\cos(\theta)/\lambda$, c is the speed of sound, and λ is the wavelength, $\lambda=c/f$. Therefore, transmit CW lateral frequency response ${}^1G_t(f_x)$ is a delta function at the frequency $f_x=\sin(\theta)/\lambda$ (FIG. **6**), and it is space invariant in the region R_+ (FIG. **2**.*a*):

$${}^1G_t(f_x)=\delta\left(f_x-\frac{\sin\theta}{\lambda}\right). \quad \text{(Eq. 2)}$$

If the finite spatial extent of the aperture is accounted for, then the transmitted field is a highly collimated beam, and is well represented by the plane-wave form described above within the beamwidth and out to the Rayleigh distance. The width of the beam is well represented by the aperture width, and the diffraction distance is the so-called Rayleigh distance $Z_0=0.5\ k\ a^2$, where a is the aperture width, k is the wavenumber, $k=2\ \pi/\lambda$. For typical ultrasound imaging frequencies and aperture sizes, this distance is very large compared to typical imaging depths. For a 30 mm aperture at 5 MHz, for example, this distance is about 10 meters. Practically, then, the transmitted plane wave has the same width as the transmit aperture, and the frequency spectrum, instead of having infinitesimal width, has a finite width on the order of 1/a. As far as the concerns of the present discussion, this width is very small and the spectrum is effectively well represented by the delta function described above.

Returning to FIG. **3** (blocks **52, 58**), a set of first receive signals is received in response to the transmitted plane wave of block **50** and stored in the memory **20** of FIG. **1**. The beamformer **24** of FIG. **1** forms sets of first beams for selected image locations from the first receive signals. FIGS. **7** and **8** respectively show the effective receive apodization function ${}^1a_r(x, x_i, z_j)$ and the delay profile ${}^1\tau_r(x, x_i, z_j)$ for the image point (x_i, z_j) in the region R_+. The focusing is achieved by a conventional delay profile which is a function of the image point coordinates (x_i, z_j). The channel-independent delay offset for each image point (x_i, z_j) is set to synchronize the arrival of the echoes from image point (x_i, z_j). Note that, at the focus, the shape of the lateral frequency response is the same as the shape of the effective apodization. The effective apodization function is given by the applied apodization function and a few element dependent factors such as element sensitivity, element directivity, tissue attenuation, 1/r diffraction, etc. To achieve a RECT-shaped receive lateral frequency response, the shape of the applied apodization is set such that the shape of the effective receive apodization ${}^1a_r(x, x_i, z_j)$ is uniform. The width of the receive lateral frequency response ${}^1G_r(f_x)$ is a function of the receive f-number and wavelength (FIG. **9**):

$${}^1G_r(f_x)=\prod\left(\frac{f_x}{\frac{1}{\lambda\cdot fnumber_r}}\right), \quad \text{(Eq. 3)}$$

where π is the RECT function. Note that, assuming constant f-number and constant speed of sound in R_+, ${}^1G_r(f_x)$ is also space invariant in R_+.

The round-trip lateral frequency response of the first component beam ${}^1G(f_x)$ (FIG. **10**) is given by the convolution of the corresponding lateral frequency responses of transmit ${}^1G_t(f_x)$ and receive ${}^1G_r(f_x)$:

$${}^1G(f_x)={}^1G_t\otimes{}^1G_r=\prod\left(\frac{f_x-\frac{\sin\theta}{\lambda}}{\frac{1}{\lambda\cdot fnumber_r}}\right), \quad \text{(Eq. 4)}$$

where $\otimes$ is the convolution operator. Note that, ${}^1G(f_x)$ is centered at the transmit lateral frequency $\sin\theta/\lambda$ and has a bandwidth that is equal to the receive (one- way) bandwidth $1/(\lambda\ \text{fnumber}_r)$. It is space-invariant within the region R_+ because so are ${}^1G_t(f_x)$ and ${}^1G_r(f_x)$.

Returning to FIG. **3**, the system **10** of FIG. **1** next transmits a second substantially planar ultrasonic wave at a steering angle of $\theta_2=-\theta$ (block **54**). As shown in FIG. **11**, the transmit apodization function ${}^2a_t(x)$ is again a substantially constant function that includes all of the transducer elements. The associated transmit delay profile ${}^2\tau_t(x)$ (FIG. **12**) decreases linearly from one end of the transducer array to the other. As shown in FIG. **13**, the lateral frequency response ${}^2G_t(f_x)$ is again substantially a delta function, but this time at the frequency $-\sin(\theta)/\lambda$. Note that ${}^2G_t(f_x)$ is space invariant in the region R_-.

Returning to FIG. **3** (blocks **56** and **60**), the system **10** of FIG. **1** receives a set of second receive signals in response to the transmitted plane wave of block **54** and stores the second receive signals in the memory **22** of FIG. **1**. As before, receive signals are digitized and stored for all transducer elements. The beamformer **26** of FIG. **1** forms sets of second beams for selected image locations from the second receive signals. The receive apodization function ${}^2a_r(x, x_i, z_j)$ and delay profile ${}^2\tau_r(x, x_i, z_j)$ applied on the second set of receive signals, and the corresponding lateral frequency response ${}^2G_r(f_x)$ are shown in FIGS. **14**, **15** and **16**, respectively, and they are the same as the ones for the first set. The delay offset is again set to synchronize the arrival of the echoes from image point (x_i, z_j). The round-trip spectrum ${}^2G(f_x)$ (FIG. **16**) is centered at $-\sin(\theta)/\lambda$ and its bandwidth is also equal to the receive bandwidth $1/(\lambda\ \text{fnumber}_r)$. It is space-invariant within the region R_-:

$$ {}^2G(f_x) = {}^2G_t \otimes {}^2G_r = \prod\left(\frac{f_x + \frac{\sin\theta}{\lambda}}{\frac{1}{\lambda \cdot fnumber_r}}\right). \quad \text{(Eq. 5)} $$

Returning to FIG. **3** (block **62**), the first and second beamformed receive signals are combined by the synthesizer **28** of FIG. **1**. In this example, we will assume a synthesis function that consists of simple summation. The synthesized spectrum $G(f_x)$, then, is the summation of the spectra of the first and second component beams ${}^1G(f_x)$ and ${}^2G(f_x)$.

Given the spectra of the component beams (FIGS. **10** and **17**), a RECT shaped spectrum can be synthesized by setting the f-number of the receive apodization for each component beam equal to:

$$ fnumber_r = \frac{1}{2\sin\theta}. \quad \text{(Eq. 6)} $$

If the f-number is set less/greater than this value a null/spike is created in the middle of the round-trip spectrum. This results in undesirable spatial response with high side lobes because of the discontinuities in the spectrum. If the effective receive apodization is a tapered function instead of a RECT one, the preceding equation becomes an upper limit for the preferred f-number.

FIG. **18** shows the synthesized lateral frequency response $G(f_x)$ which is space-invariant in R, the region of overlap of R_+ and R_-. With the f-number selected based on the above equation, the shape of the synthesized spectrum is a RECT function with a bandwidth twice the component beams' bandwidth, i.e., $2/(\lambda\ \text{fnumber}_r)$:

$$ G(f_x) = {}^1G + {}^2G = \prod\left(\frac{f_x}{\frac{2}{\lambda \cdot fnumber_r}}\right). \quad \text{(Eq. 7)} $$

Since the lateral spectrum is space-invariant and has twice the one-way bandwidth, every image location in R is effectively in focus for both transmit and receive. Note that the lateral spectrum of a conventional beamformer with fixed-transmit dynamic-receive focus is space variant (dependent on the distance to transmit focus depth). Note also that, at its transmit focus depth, a conventional beamformer with RECT effective apodization shape and the same f-number on both transmit and receive would have a triangle shaped round-trip lateral spectrum with a total frequency span of $2/(\lambda\ \text{fnumber})$, i.e., it would have a 6 dB lateral bandwidth that is only half the 6 dB bandwidth of the synthesized spectrum above.

If θ_2 is not equal to $-\theta_1$, then the condition to prevent the occurrence of a null/ spike in the round-trip spectrum (assuming again a RECT effective receive apodization) becomes

$$ fnumber_r = \frac{1}{\sin\theta_1 - \sin\theta_2}. \quad \text{(Eq. 8)} $$

For the case where the f-number for the first component beam is different than the f-number for the second component beam, the condition that needs to be satisfied for no null/spike in the spectrum (assuming again a RECT effective receive apodization for both beams) is

$$ \frac{{}^1fnumber_r \cdot {}^2fnumber_r}{{}^1fnumber_r + {}^2fnumber_r} = \frac{1}{2(\sin(\theta_1) - \sin(\theta_2))}. \quad \text{(Eq. 9)} $$

where, ${}^1\text{fnumber}_r$ and ${}^2\text{fnumber}_r$ are the receive f-numbers for the first and second component beams, respectively.

Note that the f-number conditions described above for a desirable synthesized spectrum are independent of the wavelength λ (and temporal frequency f). Therefore, the CW discussion above equally applies to PW cases with arbitrary temporal frequency responses.

FIGS. **20**, **21** and **22** respectively show the simulated point spread functions associated with pulsed. transmit plane waves steered to the right (+θ), steered to the left (−θ) and the resulting synthesized beam generated by a summation synthesis function **28**. Similarly, the two-dimensional spatial spectra for the beams generated in response to the right-steered transmit plane wave, left- steered transmit plane wave and the resulting synthesized beam are shown in FIGS. **23**, **24** and **25**, respectively. In FIGS. **20**–**25** the dynamic range is 60 dB. FIG. **26** shows the beam plot (maximum projection) for the beams generated in response to the right-steered transmitted plane wave, the left- steered transmitted plane wave, and the resulting synthesized beam at **100**, **102** and **104**, respectively. FIG. **27** shows the lateral two dimensional spatial spectrum (cross section) for beams generated in response to the right-steered transmitted plane wave, the left-steered transmitted plane wave, and the resulting synthesized beam at **110**, **112** and **114**, respectively.

FIGS. **28**–**41** show another example where a triangle-shaped round-trip lateral frequency response of a total frequency span of $2/(\lambda\ \text{fnumber})$ is synthesized using a first and second set of beams (FIG. **42**). FIGS. **28**–**42** correspond to FIGS. **4**–**18**, respectively, and the foregoing discussion of FIGS. **4**–**18** can be referenced for a fuller explanation of the parameters illustrated in FIGS. **28**–**42**. This response, as discussed above, is equivalent to at-focus performance of a conventional beamformer with RECT-shaped transmit and receive effective apodization functions and identical transmit and receive f-numbers. Note that, since the desired round-trip aperture function in this example is also a symmetric one, the effective receive apodization function for the second firing (FIG. **40**) is the mirror image of that of the first firing (FIG. **33**), i.e., ${}^2a_r(x)={}^1a_r(-x)$. In general, however, the receive apodization functions for the component beams do not need to be mirror images of each other, such as in those cases where the desired round-trip aperture function is not symmetric. Note also that, from the stored sets of first and second receive signals, any round-trip aperture function of arbitrary shape can be generated by varying the receive apodization functions without any new firings.

The region R (FIG. **2***c*) over which the image locations are distributed is preferably the region over which the left and right symmetrically steered plane waves both remain substantially planar. To cover every image point in a frame, multiple pairs of plane waves with different steering angles may be used.

The techniques described here are readily applicable to two-dimensional or three-dimensional arrays for three-dimensional imaging. Since synthesizing a lateral spectrum with full round-trip bandwidth along a single lateral axis utilizes at least two planar waves with substantially different frequency components along that axis, synthesizing a 2-D lateral spectrum with full bandwidth along azimuth and elevation axes utilizes more than two transmit-receive events. The following demonstrates a preferred four plane wave method to synthesize a RECT-shaped lateral frequency response with a band area of 2/(λ f-number$_{r,x}$) by 2/(λ f-number$_{r,y}$), where f-number$_{r,x}$ and f-number$_{r,y}$ are one-way receive f-numbers in azimuth and elevation, respectively.

FIGS. **43–55** show the transmit, receive and round-trip spectra of the component beams and the spectrum of the resultant synthesized beam. The first transmitted plane wave is steered such that the angle between the x-z plane component of the direction of propagation and the z axis is θ and the angle between the y-z plane component of the direction of propagation and the z axis is ψ. The corresponding 2-D spatial spectrum is a delta function, $\delta(f_x-\sin(\theta)/\lambda, f_y-\sin(\psi)/\lambda)$ and the bird's eye view of the spectrum is shown in FIG. **43**. The second, third and fourth transmitted plane waves are steered at (θ,−ψ), (−θ,−ψ) and (−θ,ψ), respectively. The corresponding spatial spectra are shown in FIGS. **44**, **45** and **46**, respectively. The received signals in response to each of these transmissions are digitized and stored on all acquisition channels. For an image point at (x_i,y_j,z_l), where (x_i,y_j,z_l) is in the volume insonified by all four plane waves, the applied 2-D receive apodization is selected such that the effective receive apodization is a RECT function. The aperture sizes in the x and y axes are selected such that $\text{fnumber}_{r,x}=1/(2\sin(\theta))$ and $\text{fnumber}_{r,y}=1/(2\sin(\psi))$. The receive spatial spectrum for each component beam, then, is a RECT function (FIGS. **47–50**) with a 2 sin(θ)/λ by 2 sin(ψ)/λ (or, 1/(λ fnumber$_{r,x}$) by 1/(λ fnumber$_{r,y}$)) rectangular band area. The round-trip spectra for the four component beams are given by the 2-D convolution of the respective transmit and receive spectra, and are shown in FIGS. **51–54**. If the four component beams are coherently summed to form the synthesized beam, then the resultant spectrum is also a RECT function with a 4 sin(θ)/λ by 4 sin(ψ)/λ (or, 2/(λ fnumber$_{r,x}$) by 2/(λ fnumber$_{r,y}$)) rectangular band area (FIG. **55**).

Note that some of the substantial imaging benefits that are enabled by this invention are also available in a simplified implementation (referred to below as a "reduced implementation") that may be implemented in current ultrasound imaging systems without drastic architectural changes. In this reduced implementation there are two separate transmit firings used for each ultrasound line and receive signals are apodized using apodization functions that preferably vary with the steering angle of the respective plane waves as described above. The transmitters are configured to fire a pair of plane waves that are angled with respect to the line, and the receive beamformer is configured to dynamically track the transmit field as it traverses the line. The streams of line data that result from these two firings may simply be added to result in the final synthesized line data, or other methods of combination of the data, pre and/or post-detection, may be used. Note that architectures that support aperture synthesis would support such processing. This line data may then be processed in standard fashion, including splicing this line data with otherwise acquired line data. While this reduced implementation does not result in the large frame-rate benefit that is enabled by the preferred technique described above (this approach acquires a line of data with two firings where the earlier described approach acquires an image or a section of an image with two firings), it does result in the generally high lateral bandwidth and large depth-of- field that is associated with the preferred technique. Therefore, this technique can replace the technique currently used to increase the depth-of-field which uses 3 to 8 transmit/receive events per ultrasound line, each one focusing at a different depth.

This reduced implementation may also be used to produce multiple receive beams. Since the transmit beams are focused beams in the conventional beamformation techniques, the receive beams must be very nearly collinear with the transmitted beam or the round-trip locus of sensitivity becomes distorted in the vicinity of the transmit focus and imaging artifacts result. To remedy this problem, various techniques such as limiting the number of receive beams per transmit beam, reducing the receive beam spacing, widening the main lobe of the transmit beam, predetection filtering, etc., have been used. These techniques result in either under-utilization of the processing power of the multiple beamformer, or lateral resolution compromise, or both. However, since the transmitted field with the plane wave techniques described above is highly uniform in space, the round-trip locus of sensitivity is determined by the receive beam alone. Therefore, as many receive beams as multiple beamformers can form in parallel can be formed without introducing image artifacts, i.e., the processing power can be used fully. In addition each synthesized beam enjoys full lateral bandwidth and large depth-of-field. The delay data associated with each receive beam and each transmit firing are preferably arranged such that each receive beam tracks the transmit pulse as it traverses the line. As multiple receive beams are generally focused along different lines, the delay data associated with each beam will generally differ. What's more, the delay data associated with any particular line will generally differ between the two transmit firings because the angled plane wave excitation occurs at different times for spatially distinct lines.

Note that in another variant of this reduced implementation, the two plane waves may be fired simultaneously. While such an approach has the added benefit of a factor of two increase in frame-rate, it does not allow the use of the left-right inverted pairings of receive apodization functions. As outlined above for the case of the full implementation, the preferred embodiment of these reduced implementations includes the use of an effective receive aperture size that is related to the transmitted plane wave steering angles. Note also that the dynamic receive delay profiles evolve more rapidly than standard delay profiles. This is because under angled plane wave excitation, the point at which the transmitted plane waves intersect the ultrasound line migrates out in range at a velocity that is larger than the sound speed by a factor of 1/cos(θ), where θ is the angle between the ultrasound line and the normal to the plane wavefront. Likewise, the f-number associated with the receive aperture is preferably related to the transmitted plane wave angle by about 1/(2 sin(θ)) (for the case where $|\theta_1|=|\theta_2|=\theta$).

There is also an approximate form of this single-firing method that makes use of standard receive delay profiles. Where the preferred receive delay profiles evolve to track the time at which the transmitted plane waves intersect the ultrasound line, this approximate embodiment may be implemented by modification of the transmit delay profiles only. A "depth of interest" is chosen and the transmit (plane wave) delay profiles are modified with a net delay offset such that the plane waves intersect the ultrasound line at that depth at a time that is equal to the depth divided by the sound speed. In this embodiment, standard receive delay profiles may be used. The locus of the receive focus and the intersection of the plane waves and the ultrasound line then coincide precisely at the depth-of-interest, and coincide to a degree that degrades with distance from the depth-of-interest.

Other variants make use of the fact that various signal parameters may be varied across the plane wavefront by variation of those parameters on an element-by-element basis in the transmitters. Because different parts of the plane wavefront intersect the ultrasound line at different depths, this parameter variation gets mapped onto depth. The signal can therefore be optimized for imaging at various depths. As an example, consider a left-steered plane wave that was launched by a series of elements, where the frequency that each element radiates is gradually lowered from the left-most to the right-most element. Then the radiated planar wavefront will have a gradual frequency shift in which the left side of the plane wavefront has a higher frequency than the right side. That is, it is frequency modulated across the wavefront. Because the left side of the plane wavefront crosses the ultrasound line of interest at a more shallow depth than does the right side of the plane wavefront, the insonification frequency along the ultrasound line is lower at large depths than it is at more shallow depths. Such a scheme may be used in conjunction with a depth dependent receive filter to enhance penetration. Envelope amplitude (transmit apodization) can also be varied across elements, for example, to compensate for the elevation diffraction effects on 1-D arrays to achieve field strength that is uniform with depth. Envelope bandwidth, in addition, may be modulated across elements (and therefore across depths) such that larger depths are insonified by larger duration pulses. Such pulses are more resistant to attenuation-induced frequency shifts than are wider band pulses and therefore additionally benefit penetration. Such pulses may also contain more overall energy (depending upon what is limiting the transmitted power). If a coded transmit pulse such as a chirp is used, the coding may be made more aggressive with depth. Such a scheme would again contribute to penetration at depth. The pulse used for shallow depths could be made a conventional (non-coded) pulse which evolves gradually into an aggressively coded pulse at depth, which would obviate problems associated with imaging at shallow depths with large duration transmit codes.

Other parameters may be varied on a firing-by-firing basis. The left-steered plane wave, for example, may be fired with a phase offset relative to the right- steered plane wave. If this phase offset is close to one half of a fundamental cycle, then the resultant fundamental frequency signal components combine destructively in each of the resultant beams but the second harmonic signal components generated during propagation add constructively. The resultant fundamental suppression is advantageous for second harmonic imaging. If the phase difference is close to a quarter of a fundamental cycle, then the second harmonic component that is generated via propagation distortion is suppressed. This has advantage in second harmonic imaging of ultrasound contrast agents (see U.S. application Ser. No. 09/191,034, assigned to the assignee of the present invention, for further information on this technique).

In all of the above implementations non-planar waves can also be used. For example, weakly diverging waves with substantially different wavefront angles can be used to cover a wider overlap region R per pair of transmit/receive events. This results in an SNR loss which may be recovered by using coded pulses with high time-bandwidth products on transmit and decoding on receive. Note that an unfocused wave does not have to be characterized by a single virtual line/point source behind the transducer, as in the case of cylindrical/spherical waves, and may instead have a distributed set of virtual line/point sources. Weakly focused waves can also be used for a higher signal to noise ratio while compromising the area of the overlap region R, i.e. compromising the field of view, and therefore, frame rate. Similarly, a weakly focused wave does not have to be characterized by a single focus point but by a distributed set of line/point foci. The transmitted fields may in fact have nearly any form, although only unfocused and weakly focused (as compared to the receive focusing) are discussed here. The transmitted waves preferably have substantially different wavefront angles and yet sufficient intensity in the image region. The appropriate receive aperture for each image location is preferably selected based on the wavefront angles of the pair of transmitted waves at that location.

The synthesized lateral bandwidth is generally at its broadest when the two firings are at the largest possible angle with respect to one another, but smaller angles are advantageous under some imaging conditions, such as when non-uniform tapered receive apodizations are used (see below). The largest possible angle is determined by the minimum practical SNR. The more highly steered the beam, the lower the transmitted signal level (owing to single-element radiation roll-off as well as other factors such as obliquity), and the worse the SNR.

At a particular imaging point, the structure of the transmitted wave may be considered to be substantially planar. This is true because the focused receive beam will generally select only the transmitted wave in the vicinity of the image point. Because the transmitted wave is unfocused (or weakly focused compared to the receive focusing), the receive beam structure dominates the transmit wave structure. The transmitted wave is substantially equivalent to a plane wave that is steered at some angle θ_1 with respect to a locally defined angle. A plane wave is a very narrowband excitation in the lateral spatial sense. The effective transmit spectrum at this image point is very much like a delta function at a spatial frequency of $\sin(\theta_1)/\lambda$. For the second firing, the local angle is θ_2 and the associated delta-like spectral structure is located at a spatial frequency of $\sin(\theta_2)/\lambda$. In this sense, the transmitted field is, for a particular field point of interest, effectively planar regardless of its larger-scale structure.

The receive apodizations associated with this pair of transmitted fields are preferably selected such that the resultant synthesized round-trip spatial frequency spectrum (and therefore point-spread-function) has acceptable structure. The round-trip spatial frequency spectrum associated with the first transmission is given by the convolution of the spatial frequency spectra associated with transmit and receive. Since the spectrum of the transmit field is effectively delta-like, the round trip spectrum will be very much like a shifted copy of the receive spatial frequency spectrum (which has the same functional form as the receive apodization). The same is true of the round-trip spectrum associated with the second firing.

Consider first the case in which the receive apertures are unsteered. In that case the round-trip spectrum associated with the first transmission is, like the effective transmit spectrum, centered at the spatial frequency $\sin(\theta_1)/\lambda$, and the functional form is that of the receive aperture used in the first firing. The second is centered at $\sin(\theta_2)/\lambda$ and has the functional form of the second receive aperture. In the case when the synthesis is simply additive, the full round-trip spectrum is simply the sum of these two contributing round-trip spectra. For a reasonable resultant synthesized spectrum, the two sub-spectra preferably either (1) have sharply discontinuous edges that abut one another such that they add to a continuous spectral form, or (2), overlap and be tapered in such a way that the spectral overlap adds to result in a smooth synthesized spectrum.

If the receive aperture associated with the first firing is steered, then the resultant round-trip sub-spectrum will not be centered at a spatial frequency of $\sin(\theta_1)/\lambda$, but will be shifted relative to that frequency by an amount determined by the receive steering angle. Regardless, the final requirement is that the sub-spectra should add to result in a smooth synthesized spectrum. In other words, the transmit angle, the receive steering, and the receive apodization associated with the second firing are chosen such that the resultant sub-spectra combine to form a desirable (i.e., smooth) final spectrum.

For any pair of transmitted field angles there are a number of viable receive apertures. Some examples may be helpful. Consider the case outlined earlier in which the transmitted field is a pair of plane waves launched at equal but opposite angles and the receive aperture is uniform and unsteered. In this case the resultant sub-spectra are uniform, and with the use of receive f-numbers given by (Eqn 6), they abut one another to result in a smoothly adjoined, very broad round-trip synthesized spectrum. An alternative would be to use triangular receive apertures with twice the width of the uniform ones. In such a case the resultant sub-spectra are triangular and overlap over half their widths to result in a trapezoidal synthesized spectrum. Another alternative would be to retain the uniform receive apertures and f-numbers but steer by equal amounts. The resultant sub-spectra would then both shift, but by equal amounts such that they still abutted and formed a smooth synthesized spectrum (note that the physical apertures would have to be widened to retain the same f-number due to obliquity).

The insonification angles that come about in the case of plane wave transmit waves are particularly simple in that the wavefront angles are, over a fairly large region, independent of position. For any particular image point, however, a wide variety of different transmit waves that are non-planar result in the same pair of insonification angles at the point of interest. Single element transmit apertures at ($-d \tan \theta$) and ($d \tan \theta$), for example, where d is the depth of the image point and the positions are relative to the point on the transducer where the normal intersects the point of interest, results, for a linear transducer, in insonification angles of $+/-\theta$. Note that in the above discussion the only consideration with regards to the transmitted wave is the wavefront angle of that wave at the imaging point in question. This angle is determined primarily by the delay profile (and to some degree by the frequency). Generally any delay profile may be used, though, as was mentioned earlier, the pair of waves that result in a large angular difference in wavefront angle is generally the best pair, up to the point of SNR concern. The pulse design is for the most part incidental to the lateral concerns, except inasmuch as the frequency affects the determination of the angle.

In some cases it may be desirable to make use of more than two transmit/receive events per 2-D image image point (or, more than four transmit/receive events per 3-D image point). If, for example, the ultrasound system does not have as many receive channels as the probe has elements, the minimum receive f-number and, therefore, the maximum receive spatial bandwidth achievable at deep depths are limited. In these cases, using an unsteered wave, that corresponds to a delta function at D.C. in the spatial spectrum, in addition to the left- and right-steered waves ($+-\theta$), would allow synthesizing a contiguous bandwidth of $3 \sin(\theta)/\lambda$ with receive f-numbers as high as $1/\sin(\theta)$. The same general guidelines presented above for the two-transmission case are preferably followed when more than two firings with different angles are used: the receive aperture associated with each firing is such that the round trip spectra either (1) have sharply discontinuous edges that abut one another to yield a continuous synthesized spectrum, or (2) have tapered edges that overlap one another in such a way that the synthesized spectrum is reasonably continuous. Again, the sets of receive aperture widths, receive apodizations, and local angles associated with the transmitted fields are the important parameters in the design. As the synthesized lateral spectrum determines the lateral beam structure, these parameters are preferably chosen to yield a spectrum that is associated with desirable lateral beam structure.

The image can be formed on an arbitrary sampling grid. In FIG. **56** the image locations **120** are located on a rectangular grid. In FIG. **57** the image locations **120** are oriented along radiating lines, in many ways similar to the location of beamformed receive signals organized on conventional receive scan lines. This type of grid may be used to compensate for spatial variations in the Nyquist sampling rate. The sampling grid may also be made equal to the display grid, thereby eliminating the need for scan conversion.

The system **10** can maximize the spatial bandwidth while achieving dynamic focusing on both transmit and receive. In other words, the system **10** can form images with effective round-trip aperture functions that are as wide as twice the maximum one-way aperture and have a RECT shape.

In addition to maximizing the spatial bandwidth, the system **10** also maximizes the temporal bandwidth because all the spatial information necessary to form a frame (or volume) of image (with maximum spatial bandwidth) can be acquired with only a few transmit/receive events. Therefore, the frame rate is no longer limited by the time required to transmit along and receive from hundreds of different angles or lines, but by the processing bandwidth of the receive beamformer. Thus, the technique described above eliminates the fundamental limit to dynamic, very-high-frame-rate, two- and three-dimensional imaging.

The effective round-trip apodization function achieved with the system **10** is not limited to the RECT shape. Alternatively, the effective round trip apodization function can be shaped to an arbitrary shape by applying appropriate apodization during receive beamformation. Since beamformation is done on the stored receive signals, multiple images with different aperture functions can be formed using the same data. These images can be processed differently and then combined to improve the information or presentation of the information.

The multiple components of the synthesized beam can be used also to detect and compensate for refraction or partial blockage of the aperture, thereby reducing shadowing.

The system **10** is compatible with conventional techniques such as sliding aperture, synthetic aperture, coded excitation, spatial compounding, frequency compounding, adjacent element shorting, and the like.

All conventional imaging modes can be used with the present invention to achieve the benefit of increased frame rates. For example, modes such as Color Doppler (velocity, power, etc.) which require multiple insonifications from each resolution cell can now operate at a much higher frame rate. Operations that are inherently low in signal to noise ratio, such as tissue harmonic imaging in the absence of contrast agent, may not provide optimum results with unfocused or weakly focused transmit waves. For these operations, the system **10** may be modified to be operated as a conventional, multiple-receive beamformer forming transmit beams along ultrasound lines.

If the object being imaged moves during the transmit/receive events, the respective component beams may be motion compensated (spatially aligned) before the synthesis, if desired.

It will be understood that the system described above includes memories that store receive signals received on all acquisition channels for a few firings. In order to achieve an extremely high frame rate, a receive beamformer with a very high processing bandwidth is desirable. However, these characteristics are not long-term problems, in view of the rapidly advancing technology for larger and cheaper memory and increased processing bandwidth.

The term "image location" is used broadly to refer to a point or to a region around a point.

The term "sum" is intended to encompass weighted sums.

The terms "substantially simultaneous" or "simultaneous" are used for transmit firings that cause received echoes to overlap in time.

The term "set" is intended to mean one or more.

The term "receive signal" is applied to signals at any stage of processing between the transducer elements and the output of the receive beamformer.

The term "beam" is intended to mean in the broadest sense the coherent sum of receive signals from at least two receive channels. Except in very few special cases, signals from different channels are first delayed and weighted relative to each other before they are coherently summed to form a beam. Thus, a beam may include only a coherent sum for a single image location, and the term "beam" is not limited to a series of coherent sums for image locations arranged along a line such as a scan line.

Of course, it will be apparent that many changes and modifications can be made to the preferred embodiments described above. As discussed above, a wide variety of techniques can be used to implement the various signal processing components of the disclosed system.

The foregoing detailed description has discussed only a few of the many forms that the present invention can take. For this reason, this detailed description is intended by way of illustration and not limitation. It is only the following claims, including all equivalents, that are intended to define the scope of this invention.

REFERENCES

[1] Jeong, M. K. et al., "Generation of Sinc Wave by a One-Dimensional Array for Application in Ultrasonic Imaging", IEEE Transactions on Ultrasonics, Ferroelectrics, and Frequency Control, Vol. 43, No. 2, 285–295, March 1996.

[2] Jeong, M. K. et al., "Realization of Sinc Waves in Ultrasound Imaging Systems" Ultrasonic Imaging, 21, 173–185, 1999.

[3] Lu, J., "Experimental Study of High Frame Rate Imaging with Limited Diffraction Beams", IEEE Transactions on Ultrasonics, Ferroelectrics, and Frequency Control, Vol. 45, No. 1, 84–97, January 1998.

What is claimed is:

1. A medical ultrasonic imaging method for insonifying contrast agent, said method comprising:

(a) introducing a contrast agent into a tissue; and then

(b) directing a set of substantially planar ultrasonic wavefronts at the contrast agent with a phased array transducer comprising a plurality of transducer elements.

2. The method of claim **1** further comprising

(c) receiving echo signals of said set of substantially planar wavefronts of (b); and

(d) generating an image from said echo signals of (c).

3. The method of claim **1** wherein the contrast agent of (a) comprises microbubbles.

4. The method of claim **1** wherein the set of substantially planar wavefronts comprises at least two substantially planar wavefronts travelling in separate respective directions in the tissue and overlapping in time.

5. The method of claim **1** further comprising:

(c) directing a second set of substantially planar ultrasonic wavefronts at the contrast agent with the transducer after (b), wherein the first-mentioned and second sets of wavefronts differ in at least one of the following transmit parameters: envelope modulation frequency, envelope amplitude, envelope amplitude profile, envelope phase and envelope phase profile.

6. The method of claim **5** further comprising:

(d) acquiring first and second sets of receive signals in response to the first and second sets of wavefronts, respectively; and

(e) forming an image signal as a function of both the first and second sets of receive signals.

7. The method of claim **1** further comprising:

(c) directing a second set of substantially planar ultrasonic wavefronts at the contrast agent with the transducer; and

(d) acquiring first and second sets of receive signals in response to the first and second sets of wavefronts, respectively, wherein the first and second sets of receive signals differ in at least one of the following receive parameters: apodization function, demodulation frequency, envelope amplitude, envelope amplitude profile, envelope phase, and envelope phase profile.

8. The method of claim **7** further comprising:

(e) forming an image signal as a function of both the first and second sets of receive signals.

9. The method of claim **7** or **8** wherein the first-mentioned and second sets of wavefronts differ in at least one of the following transmit parameters: envelope modulation frequency, envelope amplitude, envelope amplitude profile, envelope phase and envelope phase profile.

10. The method of claim **1** wherein the set of wavefronts of (b) comprises multiple wavefronts simultaneously travelling through the tissue.

* * * * *

patsnap

专利名称(译)	用于形成医学超声图像的方法和设备

公开(公告)号	[US6517489](US6517489)	公开(公告)日	2003-02-11
申请号	US09/839709	申请日	2001-04-19

[标]申请(专利权)人(译)	阿库森公司
申请(专利权)人(译)	ACUSON CORPORATION
当前申请(专利权)人(译)	西门子医疗解决方案USA，INC.
[标]发明人	PHILLIPS PATRICK J USTUNER KUTAY F BRADLEY CHARLES E THOMAS LEWIS J NAPOLITANO DAVID J
发明人	PHILLIPS, PATRICK J. USTUNER, KUTAY F. BRADLEY, CHARLES E. THOMAS, LEWIS J. NAPOLITANO, DAVID J.
IPC分类号	G01S15/00 G01S15/89 G01S7/52 A61B8/14
CPC分类号	G01S7/52026 G01S15/8959 G01S15/8909 G01S7/52049
外部链接	Espacenet USPTO

摘要(译)

医学超声成像方法使用透射平面波或基本上平面的透射波前，通过产生在深度上更均匀的峰值压力来改善造影剂成像。取决于造影剂的类型，返回的感兴趣频率和非线性响应的期望强度，可以在基本相同的时间产生多个波前以增加峰值压力。